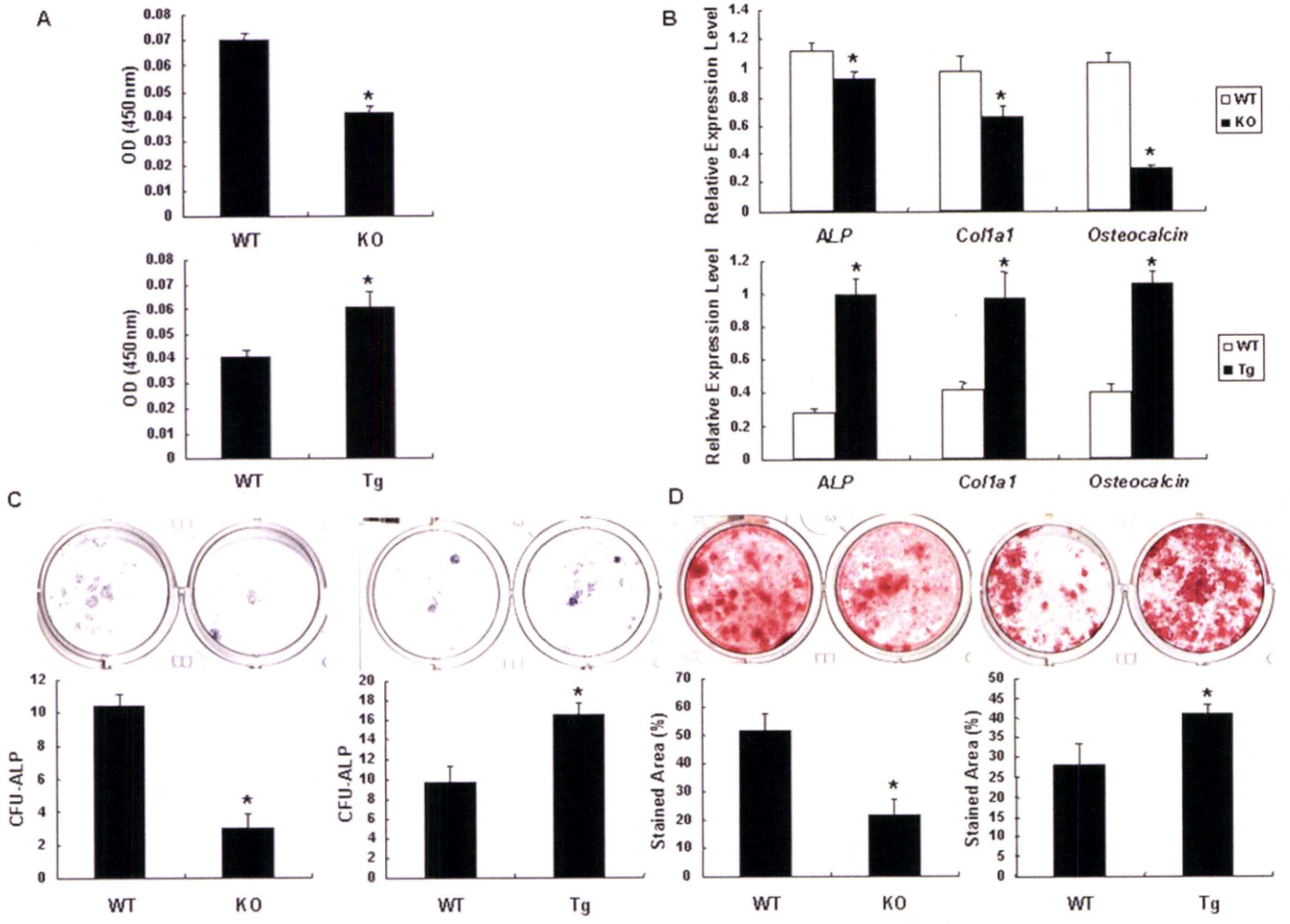

Figure 4. Effects of Cthrc1 on osteogenesis. (A) Cell proliferation in primary osteoblasts harvested from *Cthrc1*-null mice (upper panel) and from *Cthrc1* transgenic mice (lower panel) as shown by BrdU incorporation assays. (B) Expression of early and late osteoblast marker genes in primary osteoblasts harvested from *Cthrc1*-null mice (upper panel) and *Cthrc1* transgenic mice (lower panel). (C) The total numbers of CFU-ALP in bone marrow cell cultures derived from *Cthrc1*-null mice (left) and *Cthrc1* transgenic mice (right). (D) The mineralized area of CFU-O in bone marrow cell cultures derived from *Cthrc1*-null mice (left) and *Cthrc1* transgenic mice (right). WT: wild-type mice; KO: *Cthrc1*-null mice; Tg: *Cthrc1* transgenic mice. Data are shown as the mean±SEM ($^{*}p<0.05$).
doi:10.1371/journal.pone.0003174.g004

Cthrc1 in PAC1 cells, smooth muscle cell line, reduced mRNA levels of *Col1a1*, and collagen deposition [13,14]. These results suggest that the function of Cthrc1 differs among cell types, or that Cthrc1 signals through its own signaling pathway which is functional in a cell-type specific manner. In addition, there are discrepancies of phenotypes between *Cthrc1* transgenic mice which we generated in this study and the transgenic mice overexpressing *Cthrc1* previously reported [14]. First, transgenic mice we generated display a high-bone-mass phenotype, whereas transgenic mice previously reported show an osteopenic phenotype. Second, transgenic mice previously reported are smaller in size and have a higher rate of postnatal mortality, whereas transgenic mice we generated are fertile and normal in appearance and body weight. A possible explanation for these discrepancies is that transgenic mice we generated overexpress *Cthrc1* specifically in osteoblasts under the control of the *Col1a1* 2.3kb osteoblast-specific promoter to focus on the function of Cthrc1 in bones, while transgenic mice previously reported ubiquitously overexpress *Cthrc1* under the control of cytomegalovirus promoter.

Ovariectomy leads to a deficit in bone mineral densities due to cortical bone modeling and resorption of cancellous bone [19,20]. This change largely results in severe cancellous osteopenia. Dempster et al. demonstrated that the primary mechanism of ovariectomy-induced bone loss is osteoclast perforation and removal of the trabecular plates [21]. Furthermore, a recent study showed that selective ablation of estrogen receptor α in differentiated osteoclasts induced trabecular bone loss, similar to the osteoporotic bone phenotype, caused by inhibition of osteoclast apoptosis [22]. Thus, ovariectomy-induced bone loss, a model of postmenopausal osteoporosis, results from an acceleration of osteoclastic bone resorption, followed by high bone turnover in which bone resorption exceeds bone formation. *Cthrc1*-null mice exhibit cancellous bone loss, and *Cthrc1* transgenic mice increase cancellous bone with no change in osteoclastic bone resorption. In addition, Cthrc1 stimulates osteoblast proliferation and differentiation and increases bone formation rates, suggesting that Cthrc1 prevents cancellous bone loss in ovariectomized mice by stimulating osteoblastic bone formation. Indeed, bone volume and trabecular number in OVX transgenic mice were higher than those in OVX wild-type mice, and the loss of trabecular thickness by ovariectomy was protected in transgenic mice. Moreover, increased bone formation rates in transgenic mice were maintained after OVX. Considering that Cthrc1 does not affect

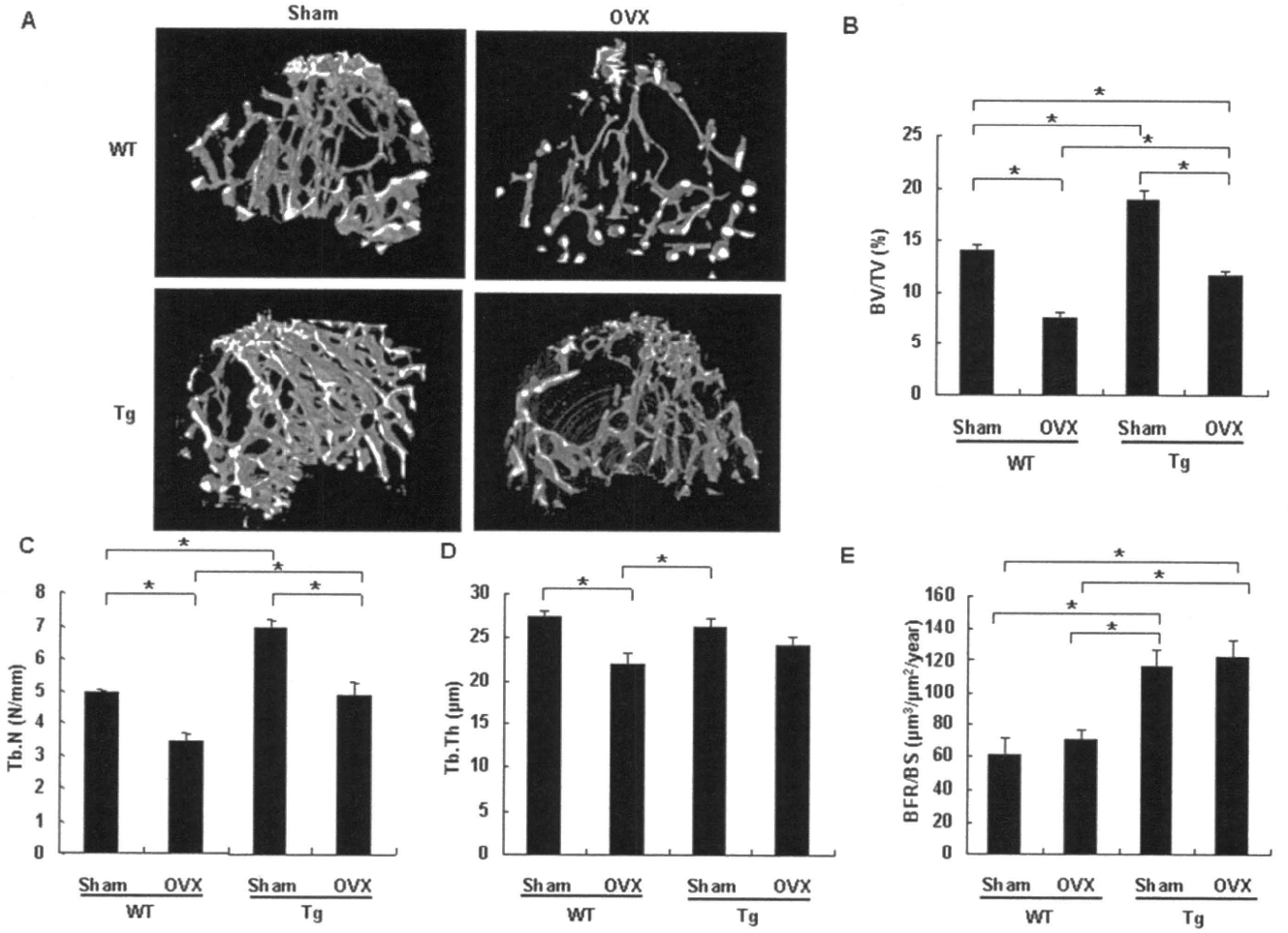

Figure 5. OVX-induced bone loss is attenuated in *Cthrc1* transgenic mice. (A) micro-CT of tibiae from 3-month-old *Cthrc1* transgenic and wild-type mice which were sham-operated or ovariectomized at 2 months of age (n = 5). (B–E) Bone volume/total volume (BV/TV) (B), trabecular number (Tb.N) (C), trabecular thickness (Tb.Th) (D) and bone formation rate (BFR) (E) were assessed by micro-CT or bone histomorphometry. WT: wild-type mice; Tg: *Cthrc1* transgenic mice. Data are shown as the mean±SEM ($^*p<0.05$).
doi:10.1371/journal.pone.0003174.g005

osteoclastogenesis, enhanced bone formation by overexpression of Cthrc1 may attenuate bone loss caused by enhanced osteoclastic bone resorption induced by OVX.

It is noteworthy in this article that Cthrc1 may have a potential role in treating osteoporosis, because we observed that osteoblast-specific overexpression of *Cthrc1* in mice attenuates bone loss which is induced by OVX, an accepted preclinical disease model of postmenopausal osteoporosis. The function of Cthrc1 as a stimulator of bone formation without affecting bone resorption is very promising, because most types of drugs which are currently used for the treatment of osteoporosis are antiresorptive in nature and insufficient for restoring bone volume in osteoporotic patients [23]. Although anabolic agents improve bone mass by stimulating osteoblast-mediated bone formation, only a single anabolic agent, parathyroid hormone 1–34 is available to treat osteoporosis at present [24,25]. Herein, we indicate that Cthrc1 attenuates estrogen deficiency-induced bone loss by stimulating osteoblastic bone formation. Hence, Cthrc1 constitutes a potential target of an anabolic therapy for osteoporosis and the therapeutic effects are expected to be enhanced with antiresorptive drugs.

Materials and Methods

Suppression subtractive hybridization

ATDC5 cells were cultured for a total of 5 days in DMEM/Ham's F12 medium supplemented with 5% FBS and 10 μg/ml insulin with medium change every other day. Cells were exposed to 1 μg/ml BMP2 or vehicle for 10 hr. Poly $(A)^+$ RNA was isolated from BMP2 -untreated and BMP2 -treated ATDC5 cells by a single-step method as previously described [26] and analyzed by suppression subtractive hybridization according to the manufacturer's instruction (PCR-Select cDNA Subtractions Kit, Clontech). After subtraction, the cDNAs were ligated into pCR2.1 (Invitrogen), and these subtracted cDNA libraries were further screened by differential hybridization (differential screening kit, Clontech). The cDNA fragment of approximately 500-bp expressed at a high level in BMP2 -treated ATDC5 cells was identified. Oligo (dT) primed cDNA library from poly$(A)^+$ RNA of BMP2 -treated ATDC5 cells was constructed in λZAP Express vector (Stratagene), and 1×10^6 plaques were screened with the 500-bp fragment as a probe as previously described [26].

Generation of mutant mice

A Cthrc1 genomic clone was isolated from a mouse 129SvEv genomic DNA library. The targeting vector was constructed by inserting an IRES-LacZ-pA-loxP-flanked neomycin resistance expression cassette into exon 2 of the *Cthrc1* gene. Homologous recombination in 129SvEv ES clones harboring *Protamine 1-Cre* transgenes was identified by Southern blot analysis of SacI-digested genomic DNA using 5′ and 3′ probes located outside the homology regions used for gene recombination [27]. Mouse chimeras were generated by C57BL/6 host blastocyst injection of mutant embryonic stem cell clones, and the chimeras obtained were bred with C57BL/6 mice to generate heterozygous *Cthrc1* mice. Heterozygous mutants were then backcrossed eight times with C57BL/6 mice to generate mutant mice with a C57BL/6 genetic background. We then performed RT-PCR to determine the presence of *Cthrc1* transcripts. We used the following primers of *Cthrc1* for RT-PCR, based on exon3 and exon4: 5′-CTGCG-AGTTCTGTTCAGTGG-3′ and 5′-GGGACTGAAATCGTC-AGAGG-3′. *Cthrc1* transgenic mice were generated using an osteoblast-specific 2.3-kb *Col1a1* promoter, the 1.25-kb 3×HA-tagged full-length mouse *Cthrc1* cDNA, and the 240-bp SV40 polyadenylation signal [28]. DNAs were injected into pronuclei of fertilized C57BL/6×DBA/2 hybrid eggs, and the injected eggs were then transferred into CD1 foster mothers. Hemizygous mutants were backcrossed eight times with C57BL/6 mice to generate transgenic mice with a C57BL/6 genetic background. The tissue specificity of transgene expression was examined in immunohistochemistry studies. Routine mouse genotyping was performed by PCR. The following primer pairs were used: 5′-CATCAAGATGGTATAAAAGG-3′ and 5′-GCAGCAGCAG-CACAAGGAAG-3′. The experimental protocols were approved by the Animal Care and Use Committee of Kyoto University.

Histological analyses

Whole mount X-gal staining of embryos was performed as previously described [29]. For the histological analyses, we fixed embryos with 4% paraformaldehyde, embedded them in paraffin, and sectioned them into 7-μm-thick slices. Immunohistochemical staining was performed using peroxidase chromogens (Zymed)/TrueBlue substrate (KPL) with rabbit polyclonal anti-HA antibody (1:500, Covance). For *in vivo* BrdU labeling, 1-week-old mice were injected intraperitoneally with 100 μg/kg BrdU (Amersham) and sacrificed 3 hr later. Sections were stained with anti-BrdU antibody (Amersham) and were counterstained with hematoxylin according to the manufacturer's instruction.

Micro-CT Analyses

High-resolution micro-CT scanning (SMX-100CT; Shimazu) was performed to measure morphological indices of metaphyseal regions of tibia as previously described [30]. Metaphyseal regions were scanned 100 times with a slice increment of 8 μm. The most proximal slice was defined as the plane where the growth plate had just disappeared. Material properties were calculated using a commercial software package (VG Studio Max1.2: Visual Science) [30].

Bone Histomorphometry

The mice were injected subcutaneously with calcein (20 mg/kg body weight; Sigma) 10 and 3 days before sacrifice. Fifth lumber vertebrae were fixed with 4% paraformaldehyde for 18 hr at 4°C. Undecalcified bones were embedded in methylmethacrylate, and 4-μm-thick sections were prepared for bone histomorphometric analyses of adult mice as previously described [31]. Sections were stained with 1% toluidine blue. Static and dynamic histomorphometric analyses were performed according to standard protocols using Histometry RT (SYSTEM-SUPPLY) [32,33].

Osteoblast Isolation and Culture

Primary osteoblasts were harvested from calvaria of newborn mice by sequential collagenase digestion (Roche) and were maintained in α-MEM containing 10% FBS. BrdU incorporation was measured using the cell proliferation ELISA Biotrack kit (Amersham).

Real-Time PCR

Primary osteoblasts were cultured in α-MEM containing 10% FBS, 50 μg/ml ascorbic acid, and 10 nM β-glycerophosphate for 10 days, and total RNA was isolated from the cultured cells by RNeasy Mini Kit (Qiagen) according to the manufacturer's instruction. Two μg of total RNA was reverse transcribed to cDNA with the use of Transcriptor First Strand cDNA Synthesis Kit (Roche). Real-time PCR was performed using the LightCycler system with the FastStart DNA Master SYBR Green (Roche). The following primers were used: *G3pdh*, 5′-TGTCCGTCGTGGAT-CTGAC-3′ and 5′-CCTGCTTCACCACCTTCTTG-3′; *ALP*, 5′-ACTCAGGGCAATGAGGTCAC-3′ and 5′-CACCCGAGT-GGTAGTCACAA -3′; *Col1a1*, 5′-CTCCTGGCAAGAATGGA-GAT-3′ and 5′-AATCCACGAGCACCCTGA-3′; *Osteocalcin*, 5′-AGACTCCGGCGCTACCTT-3′ and 5′-CTCGTCACAAG-CAGGGTTAAG-3′.

Measurement of CFU-ALP and CFU-O

Bone marrow cells were isolated as previously described [26]. Bone marrow cells from 5-week-old mice were plated into 12-well plates at 2.5×10^6 cells per well for CFU-ALP assays and at 5×10^6 cells per well for CFU-O assays, and were cultured in α-MEM containing 10% FBS, 50 μg/ml ascorbic acid, and 10 nM β-glycerophosphate. For CFU-ALP assays, cultures were stained at day 10 with Sigma alkaline phosphatase kit (Sigma), and colonies with >20 cells were counted. Cultures were stained with 1% alizarin red S (Wako) at day 20 for the CFU-O assay of *Cthrc1*-null mice, and at day 16 for that of *Cthrc1* transgenic mice, respectively. The stained area was calculated using the freeware Image-J (NIH).

Ovariectomy

Mice were ovariectomized or sham-operated at 2 months of age, and all of the mice were killed 4 weeks later and the tibiae and vertebrae were removed for analyses.

Statistical analyses

Statistical analysis was performed by Student's t test to determine the significance between groups. Wild-type and transgenic OVX and sham-operated mice were analyzed by ANOVA followed by Fisher's protected least significant difference. Values were considered statistically significant at $p<0.05$.

More methods were shown in Supporting Information Text S1.

Supporting Information

Figure S1 Analyses of Cthrc1 expression in vitro and in vivo by northern blot and in situ hybridization. (A) Effect of BMP2 (1 μg/ml) on Cthrc1 expression in ATDC5 cells. Cthrc1 expression is upregulated by BMP2. (B) Expression of Cthrc1 in various cell lines. (C) Expression of Cthrc1 in adult mouse tissues. (D) In situ hybridization analysis of Cthrc1 expression in limb buds of E13.5

and E16.5 mouse embryos. (E) Expression of Cthrc1 during embryogenesis.
Found at: doi:10.1371/journal.pone.0003174.s001 (8.89 MB TIF)

Figure S2 Skeletal preparation of Cthrc1-null and Cthrc1 transgenic mice. (A) Whole-mount X-gal staining of heterozygous Cthrc1 embryos during embryogenesis. (B and C) Skeletons of newborn Cthrc1-null mice (B) and Cthrc1 transgenic mice (C) stained by alcian blue followed by alizarin red. WT: wild-type mice; KO: Cthrc1-null mice; Tg: Cthrc1 transgenic mice.
Found at: doi:10.1371/journal.pone.0003174.s002 (5.91 MB TIF)

Figure S3 In situ hybridization analyses of osteoblast and chondrocyte marker genes in Cthrc1-null and Cthrc1 transgenic mouse embryos. Runx2, Col1a1, Col2a1 and Col10a1 expression in humeri of E16.5 embryos. (A) Cthrc1-null mouse embryos. (B) Cthrc1 transgenic mouse embryos. WT: wild-type mice; KO: Cthrc1-null mice; Tg: Cthrc1 transgenic mice.
Found at: doi:10.1371/journal.pone.0003174.s003 (10.15 MB TIF)

Figure S4 Effect of Cthrc1 on osteoclastogenesis. (A) TRAP staining of vertebrae of 2-month-old Cthrc1-null and wild-type mice. TRAP-positive osteoclast number/bone surface (Oc.N/BS) and osteoclast surface/bone surface (Oc.S/BS) are shown (n = 6). (B) Expression of RANKL in primary osteoblasts harvested from Cthrc1-null mice, assessed by real-time PCR. (C) TRAP staining of vertebrae of 2-month-old Cthrc1 transgenic and wild-type mice. TRAP-positive osteoclast number/bone surface (Oc.N/BS) and osteoclast surface/bone surface (Oc.S/BS) are shown (n = 6). (D) Expression of RANKL in primary osteoblasts harvested from Cthrc1 transgenic mice, assessed by real-time PCR. WT: wild-type mice; KO: Cthrc1-null mice; Tg: Cthrc1 transgenic mice. Data are shown as the mean±SEM (*$p<0.05$).
Found at: doi:10.1371/journal.pone.0003174.s004 (9.83 MB TIF)

Text S1 Supplementary Methods.
Found at: doi:10.1371/journal.pone.0003174.s005 (0.05 MB DOC)

Acknowledgments

We thank Janie Finch for editorial assistance, Neung-Seon Seo and Magnus Hook for technical support, and Steve O'Gorman for PC3 mouse ES cells.

Author Contributions

Conceived and designed the experiments: BdC HA. Performed the experiments: HK KMK BGD HA. Analyzed the data: HK BGD RRB TN HA. Contributed reagents/materials/analysis tools: ZZ JMD RRB BdC. Wrote the paper: HK BdC HA.

References

1. Olsen BR, Reginato AM, Wang W (2000) Bone development. Annu Rev Cell Dev Biol 16: 191–220.
2. Karsenty G, Wagner EF (2002) Reaching a genetic and molecular understanding of skeletal development. Dev Cell 2: 389–406.
3. Harada S, Rodan GA (2003) Control of osteoblast function and regulation of bone mass. Nature 423: 349–355.
4. Hughes FJ, Collyer J, Stanfield M, Goodman SA (1995) The effects of bone morphogenetic protein-2, -4, and -6 on differentiation of rat osteoblast cells in vitro. Endocrinology 136: 2671–2677.
5. Abe E, Yamamoto M, Taguchi Y, Lecka-Czernik B, O'Brien CA, et al. (2000) Essential requirement of BMPs-2/4 for both osteoblast and osteoclast formation in murine bone marrow cultures from adult mice: antagonism by noggin. J Bone Miner Res 15: 663–673.
6. Kronenberg HM (2003) Developmental regulation of the growth plate. Nature 423: 332–336.
7. Abe E (2006) Function of BMPs and BMP antagonists in adult bone. Ann N Y Acad Sci 1068: 41–53.
8. Devlin RD, Du Z, Pereira RC, Kimble RB, Economides AN, et al. (2003) Skeletal overexpression of noggin results in osteopenia and reduced bone formation. Endocrinology 144: 1972–1978.
9. Wu XB, Li Y, Schneider A, Yu W, Rajendren G, et al. (2003) Impaired osteoblastic differentiation, reduced bone formation, and severe osteoporosis in noggin-overexpressing mice. J Clin Invest 112: 924–934.
10. Zhao M, Harris SE, Horn D, Geng Z, Nishimura R, et al. (2002) Bone morphogenetic protein receptor signaling is necessary for normal murine postnatal bone formation. pp 1049–1060.
11. Mishina Y, Starbuck MW, Gentile MA, Fukuda T, Kasparcova V, et al. (2004) Bone morphogenetic protein type IA receptor signaling regulates postnatal osteoblast function and bone remodeling. J Biol Chem 279: 27560–27566.
12. Yoshida Y, Tanaka S, Umemori H, Minowa O, Usui M, et al. (2000) Negative regulation of BMP/Smad signaling by Tob in osteoblasts. Cell 103: 1085–1097.
13. Pyagay P, Heroult M, Wang Q, Lehnert W, Belden J, et al. (2005) Collagen triple helix repeat containing 1, a novel secreted protein in injured and diseased arteries, inhibits collagen expression and promotes cell migration. Circ Res 96: 261–268.
14. LeClair RJ, Durmus T, Wang Q, Pyagay P, Terzic A, et al. (2007) Cthrc1 is a novel inhibitor of transforming growth factor-beta signaling and neointimal lesion formation. Circ Res 100: 826–833.
15. Durmus T, LeClair RJ, Park KS, Terzic A, Yoon JK, et al. (2006) Expression analysis of the novel gene collagen triple helix repeat containing-1 (Cthrc1). Gene Expr Patterns 6: 935–940.
16. Kalu DN (1991) The ovariectomized rat model of postmenopausal bone loss. Bone Miner 15: 175–191.
17. Wozney JM, Rosen V, Celeste AJ, Mitsock LM, Whitters MJ, et al. (1988) Novel regulators of bone formation: molecular clones and activities. Science 242: 1528–1534.
18. Tang L, Dai DL, Su M, Martinka M, Li G, et al. (2006) Aberrant expression of collagen triple helix repeat containing 1 in human solid cancers. Clin Cancer Res 12: 3716–3722.
19. Wronski TJ, Cintron M, Dann LM (1988) Temporal relationship between bone loss and increased bone turnover in ovariectomized rats. Calcif Tissue Int 43: 179–183.
20. Turner RT, Vandersteenhoven JJ, Bell NH (1987) The effects of ovariectomy and 17 beta-estradiol on cortical bone histomorphometry in growing rats. J Bone Miner Res 2: 115–122.
21. Dempster DW, Birchman R, Xu R, Lindsay R, Shen V (1995) Temporal changes in cancellous bone structure of rats immediately after ovariectomy. Bone 16: 157–161.
22. Nakamura T, Imai Y, Matsumoto T, Sato S, Takeuchi K, et al. (2007) Estrogen prevents bone loss via estrogen receptor alpha and induction of Fas ligand in osteoclasts. Cell 130: 811–823.
23. Rodan GA, Martin TJ (2000) Therapeutic approaches to bone diseases. Science 289: 1508–1514.
24. Canalis E, Giustina A, Bilezikian JP (2007) Mechanisms of anabolic therapies for osteoporosis. N Engl J Med 357: 905–916.
25. Garrett IR (2007) Anabolic agents and the bone morphogenetic protein pathway. Curr Top Dev Biol 78: 127–171.
26. Kimura H, Akiyama H, Nakamura T, de Crombrugghe B (2007) Tenascin-W inhibits proliferation and differentiation of preosteoblasts during endochondral bone formation. Biochem Biophys Res Commun 356: 935–941.
27. O'Gorman S, Dagenais NA, Qian M, Marchuk Y (1997) Protamine-Cre recombinase transgenes efficiently recombine target sequences in the male germ line of mice, but not in embryonic stem cells. Proc Natl Acad Sci U S A 94: 14602–14607.
28. Rossert J, Eberspaecher H, de Crombrugghe B (1995) Separate cis-acting DNA elements of the mouse pro-alpha 1(I) collagen promoter direct expression of reporter genes to different type I collagen-producing cells in transgenic mice. J Cell Biol 129: 1421–1432.
29. Nakashima K, Zhou X, Kunkel G, Zhang Z, Deng JM, et al. (2002) The novel zinc finger-containing transcription factor osterix is required for osteoblast differentiation and bone formation. Cell 108: 17–29.
30. Nakanishi R, Shimizu M, Mori M, Akiyama H, Okudaira S, et al. (2006) Secreted frizzled-related protein 4 is a negative regulator of peak BMD in SAMP6 mice. J Bone Miner Res 21: 1713–1721.
31. Hahn M, Vogel M, Delling G (1991) Undecalcified preparation of bone tissue: report of technical experience and development of new methods. Virchows Arch A Pathol Anat Histopathol 418: 1–7.
32. Parfitt AM (2002) Physiologic and pathogenetic significance of bone histomorphometric data. In: Coe FL, Favus MJ, eds. Disorders of Bone Miner Metabolism, 2nd ed. Philadelphia, PA, USA: Lippincott Williams & Wilkins. pp 469–485.
33. Parfitt AM, Drezner MK, Glorieux FH, Kanis JA, Malluche H, et al. (1987) Bone histomorphometry: standardization of nomenclature, symbols, and units. Report of the ASBMR Histomorphometry Nomenclature Committee. J Bone Miner Res 2: 595–610.

SPINE Volume 34, Number 16, pp 1644–1649

Evidence of Enhanced Expression of Osteopontin in Spinal Hyperostosis of the Twy Mouse

Atsuomi Aiba, MD,*† Arata Nakajima, MD, PhD,*‡ Akihiko Okawa, MD, PhD,* Masao Koda, MD, PhD,*‡ and Masashi Yamazaki, MD, PhD*

Study Design. Gene expression and protein localization of osteopontin (OPN) in spinal hyperostosis of the twy mouse by means of in situ hybridization, immunohistochemistry, and Northern blot analysis.

Objective. To verify the involvement of OPN in spinal hyperostosis in the twy mouse and elucidate its ossification pattern at molecular levels.

Summary of Background Data. OPN is a molecule that consistently colocalizes with ectopic calcification in human pathologic conditions. The twy mouse, which shows ectopic calcification of the spinal ligament resulting in hind limb paralysis, is considered to be a model for human ossification of the posterior longitudinal ligament of the spine.

Methods. Twenty-eight each of age-matched twy, heterozygote, and wild-type mice were killed at 2, 4, 8, 12, and 16 weeks old and subject to histologic and/or molecular analyses. Sections were hybridized with RNA probes for OPN and also stained with anti-OPN antibodies. Total cellular RNA was extracted from the cervicothoracic spine of each genotype at 2- and 16-week-old, and gene expression for OPN and COL10A1 was quantified by Northern blot analysis.

Results. Enhanced expression of OPN mRNA was observed in spinal hyperostotic lesions of the twy mouse, specifically in cells of the spinal ligament and chondrogenic cells in the outer layer of the anulus fibrosus. These trends were also confirmed by immunohistochemical analyses. Northern blot analysis showed that a considerable amount of OPN transcripts was detected in all genotypes at 2 weeks old, but the robust expression of OPN mRNA was maintained only in twy mice at 16 weeks old. COL10A1 transcripts were hardly detected regardless of the genotype at 16 weeks old.

Conclusion. OPN was overexpressed in the hyperostotic spinal lesions of twy mice, and the hyperostosis was induced mainly by ectopic ossification of the spinal ligament. Because OPN is considered to be an inhibitor of calcification, further studies will be necessary to verify whether OPN overexpressed in the twy mouse is functional.

From the *Department of Orthopedic Surgery, Chiba University Graduate School of Medicine, Chiba, Japan; †Department of Orthopedic Surgery, Numazu Municipal Hospital, Numazu, Japan; and ‡Department of Orthopedic Surgery, Chiba Aoba Municipal Hospital, Chiba, Japan.
Acknowledgment date: November 13, 2008. Revision date: January 30, 2009. Acceptance date: February 10, 2009.
The legal regulatory status of the device(s)/drug(s) that is/are the subject of this manuscript is not applicable in my country.
Funds were received in support of this work. No benefits in any form have been or will be received from a commercial party related directly or indirectly to the subject of this manuscript.
Supported by a Grant-in-Aid for Scientific Research from the Ministry of Education, Science and Culture of Japan.
Address correspondence and reprint requests to Masashi Yamazaki, MD, PhD, Department of Orthopaedic Surgery, Chiba University Graduate School of Medicine, 1-8-1 Inohana, Chuo-ku, Chiba 260-8670, Japan; E-mail: masashiy@faculty.chiba-u.jp

Key words: osteopontin (OPN), ectopic calcification, spinal hyperostosis, twy mouse. **Spine 2009;34:1644–1649**

The twy (tiptoe-walking Yoshimura) mouse, established in Japan in 1978 by mating siblings of the ICR strain of mice, is a mutant (gene symbol: *ttw*) showing multiple osteochondral lesions.[1] We have used this mouse as a model for ossification of the posterior longitudinal ligament of the spine (OPLL), a disorder that causes severe cervical myelopathy in humans.[2–7] The incidence of OPLL is 1.5% among the Japanese population over 50 years old. Today, OPLL is known to occur worldwide, although it continues to occur particularly in Asia. Consequently, the hyperostotic changes in the cervical vertebral cortex of the twy mouse has drawn attention as a useful model for human ankylosing spinal hyperostosis[8] and/or diffuse idiopathic skeletal hyperostosis.[9] Both disease entities are thought to be quite similar to OPLL.

We previously determined that the twy phenotype is caused by a nonsense mutation (glycine 568 to stop) in the *Npps* gene, which encodes nucleotide pyrophosphatase.[2] This enzyme regulates soft tissue calcification and bone mineralization by producing inorganic pyrophosphatase, a major inhibitor of calcification.[10–13] Thus, the hyperostotic phenotype of the twy mouse is thought to result from dysfunction of nucleotide pyrophosphatase.

Osteopontin (OPN), a secreted glycosylated phosphoprotein, is one of the major noncollagenous proteins in bone matrix. It binds with high affinity to hydroxyapatite, possibly through its asparatic acid-rich region, and it may participate in physiologic tissue mineralization.[14] In addition, OPN interacts with the vitronectin receptor ($\alpha v\beta 3$ integrin) on osteoclasts through its Arg-Gly-Asp (RGD) sequence, implicating OPN as a potentially important participant in bone resorption.[14,15] OPN is also well known as a molecule that consistently colocalizes with ectopic calcification, and is an acidic phosphoprotein normally found in bone, teeth, kidney, and epithelial lining tissues. Expression of OPN mRNA is increased under conditions of injury and disease in many tissues, and it is closely associated with calcified deposits found in numerous pathologies including atherosclerotic lesions, aortic stenosis, kidney stones, and tumors.[16] Recent *in vitro* studies support a role for OPN as an inhibitor of calcification and hydroxyapatite growth.[17–19] Conversely, the colocalization of OPN with biomineralization in hard tissues and its ability to bind and poten-

tially orient calcium[20] suggest that OPN may promote ectopic calcification *in vivo*.

Although OPN is a key molecule involved in ectopic calcification associated with normal and/or pathologic conditions, there have been no reports showing association of OPN with spinal hyperostosis, which is the most characteristic phenotype of the twy mouse. To determine the involvement of OPN in ectopic calcification of the spinal ligament in this mutant, we assessed spatial and temporal gene expression for OPN in the spine and compared its expression profile among twy, heterozygote, and wild-type mice.

■ Materials and Methods

Animals and Tissue Preparation

The animals used in this study were 28 each of age-matched twy, heterozygote, and wild-type mice that have the ICR strain. At 2, 4, 8, 12, and 16 weeks old, mice were killed under anesthesia and their cervical spine was removed after perfusion-fixation with 4% paraformaldehyde in 0.1 M phosphate buffer. These experimental procedures were approved by the Animal Care and Use Committee of Chiba University, Japan.

Samples were then dehydrated and decalcified with 20% EDTA (pH: 7.4). After decalcification, the cervical spine was bisected sagittally in the median plane. Tissues were then embedded in paraffin and midsagittal 6-μm-thick sections were cut and mounted on silane-coated slides.

Preparation of Probes

The following cDNA clones were used as hybridization probes in this study: mouse pro-α1(X) collagen (COL10A1) cDNA containing a 0.60-kb fragment and mouse osteopontin cDNA containing a 1.2-kb fragment (a gift from Dr. S. Nomura, Osaka University, Japan). Specificity of these probes was confirmed previously.[21–24]

In Situ *Hybridization*

To compare distribution of cells expressing OPN mRNA in the cervical spine of twy and wild-type mice, sections were hybridized with probes for OPN. Digoxigenin-11-uridine 5-triphosphate-labeled single-strand RNA probes (antisense and sense probes) for mouse OPN cDNA (1.2-kb) were prepared. *In situ* hybridization was carried out as previously described.[21,22,24,25] Briefly, sections were hybridized with antisense probes at 50°C for 16 hours, and signals were detected using the digoxigenin detection kit (Roche Molecular Biochemicals, Indianapolis, IN). After signal detection, sections were counterstained with methyl-green. Sense probes were used to exclude the possibility of nonspecific signals.

Immunohistochemistry

To clarify the localization of OPN in the cervical spine of twy and wild-type mice, sections were reacted with antimouse OPN rabbit antibodies (1:100; LSL, Tokyo, Japan) as previously described.[26] Signals were detected using diaminobenzidine. Counterstaining was performed with Mayer's Hematoxyline. For negative-control sections, the same procedures were used but the primary antibody was replaced by nonimmune rabbit IgG (Vectastain, Vector Laboratories, Burlingame, CA).

RNA Extraction and Northern Blot Analysis

For RNA extraction, 4 mice of each genotype were killed as described earlier at 2- and 16-week-old, and the cervicothoracic spine was harvested. Tissues were frozen immediately in liquid nitrogen and stored at −80°C until RNA isolation was performed. Total cellular RNA was extracted using TRIzol (Gibco BRL, Rockville, MD) according to the manufacturer's instructions. Twenty μg of total RNA from each sample was subjected to 1% agarose gel electrophoresis and transferred to a nylon membrane (Hybond-XL; Amersham Pharmacia Biotech, Buckinghamshire, UK). cDNA probes were labeled with ^{32}P using a random priming method. Northern blot analysis was carried out as previously described.[21–24] The density of each band on the autoradiogram was estimated by an image analyzer (Image Gauge software, version 3.1; FUJIFILM, Tokyo, Japan).

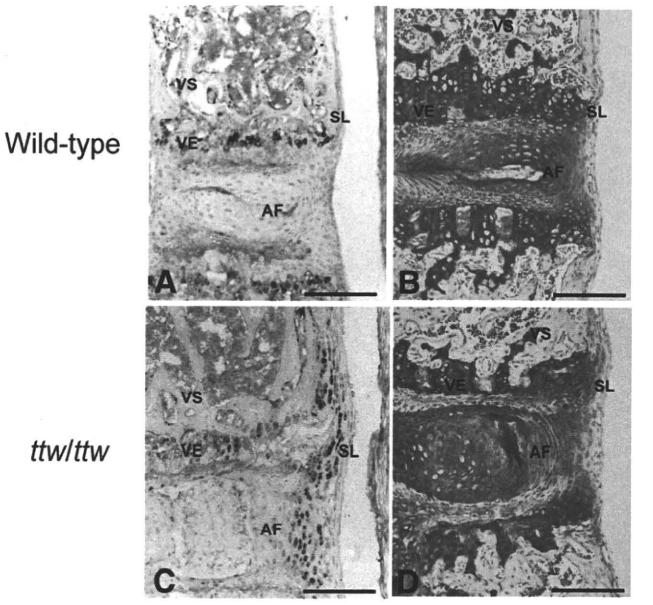

Figure 1. Expression of OPN mRNA in the cervical spine of wild-type and twy mice at 4 weeks old. In wild-type mice, expression of OPN mRNA was restricted to cells of the vertebral end plate and to osteoblasts of the vertebral primary spongiosa (**A**). In contrast, in twy mice (ttw/ttw), OPN mRNA was also detected in cells of the spinal ligament and cells of the outer layer of the anulus fibrosus (**C**). Cellular hypertrophy of these OPN mRNA-positive cells was more evident in twy mice than in the wild-type (**B, D**). VE indicates vertebral end plate; VS, vertebral primary spongiosa; SL, spinal ligament; and AF, anulus fibrosus. Scale bars = 200 μm.

■ Results

Analysis of OPN mRNA Expression by In Situ *Hybridization*

OPN mRNA was detected in cells of the vertebral end plate both in wild-type and twy mice from 2 weeks old, and there was no evident difference in its expression pattern between genotypes (data not shown).

At 4 weeks old, expression of OPN mRNA was restricted to cells in the vertebral end plate and osteoblasts in the vertebral primary spongiosa in wild-type mice (Figure 1A). In contrast, in twy mice, OPN was also detected in cells of the spinal ligament and cells in the outer layer of the anulus fibrosus (Figure 1C). Cellular hypertrophy of these OPN mRNA-positive cells was more evident in twy mice than in the wild-type (Figures 1B, D). The preferential expression of OPN in the spinal

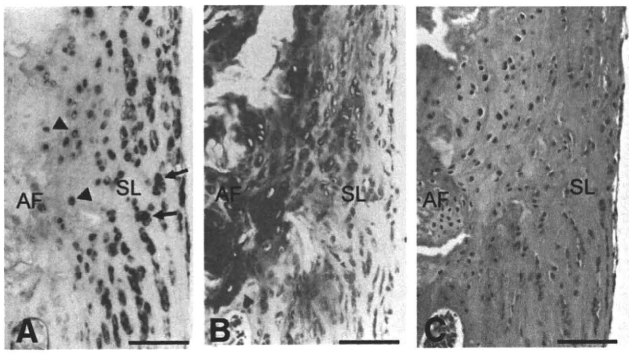

Figure 2. Expression of OPN mRNA in the posterior cervical spine of the twy mouse at 16 weeks old. Panels A to C are sequential sections. A strong OPN signal was detected in cells of the spinal ligament (**A,** arrows) and hypertrophic chondrocytes in the outer layer of the anulus fibrosus (**A,** arrowheads). The region containing OPN-positive chondrocytes in the anulus fibrosus showed metachromasia with TB staining (**B**). OPN-positive regions in the spinal ligament showed eosinophilia with HE staining (**C**). Scale bars = 50 μm.

ligament and anulus fibrosus in twy mice became more evident at 8- and 12-week-old (data not shown).

At 16 weeks old, the spinal ligament became hypertrophied in twy mice, and cells in both the posterior (Figure 2A, arrows) and anterior (Figure 4A, arrows) spinal ligaments expressed a strong signal for OPN mRNA. Hematoxyline and eosin (HE) staining revealed that these OPN-positive regions were histologically consistent with osteoid (Figure 2C). At this time point, some chondrogenic cells in the outer layer of the anulus fibrosus also expressed a strong signal for OPN mRNA (Figure 2A, arrowheads) and these regions showed metachromasia with toluidine-blue (TB) staining (Figure 2B). In contrast, the OPN signal was significantly diminished in age-matched wild-type mice (data not shown).

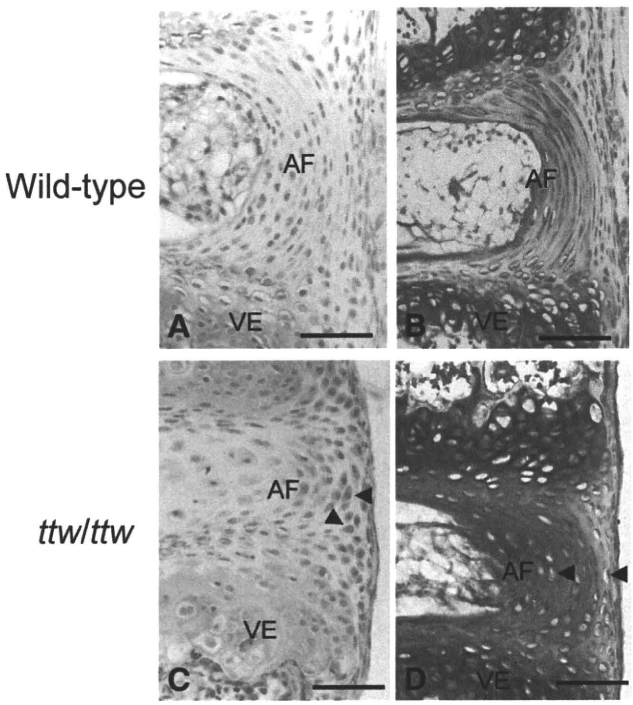

Figure 3. Localization of OPN protein in the cervical spine of wild-type and twy mice at 2 weeks old. In twy mice (ttw/ttw), OPN immunoreactivity was evident in cells of the outer layer of the anulus fibrosus. Most of the OPN-positive cells were hypertrophied and showed a round-shaped morphology (**C, D,** arrowheads). However, in wild-type mice, OPN immunoreactivity was weak and showed a spindle-shaped morphology (**A, B**). Scale bars = 50 μm.

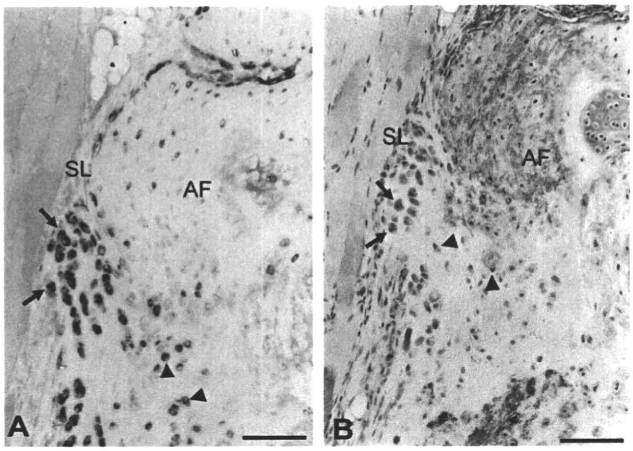

Figure 4. Expression of OPN mRNA (**A**) and localization of its protein (**B**) in the anterior cervical spine of the twy mouse at 16 weeks old. Panels A and B are sequential sections. A strong OPN mRNA signal was detected in cells of the spinal ligament (**A,** arrows) and chondrogenic cells in the outer layer of the anulus fibrosus (**A,** arrowheads). Localization of OPN protein was evident in cells that were also positive for OPN mRNA (**B,** arrows and arrowheads). Scale bars = 50 μm.

Analysis of OPN by Immunohistochemistry

At 2 weeks old, OPN immunoreactivity was detected in cells of the vertebral end plate both in wild-type and twy mice (data not shown). In addition, in twy mice, OPN was evident in cells in the outer layer of the anulus fibrosus. Most of the OPN-positive cells were hypertrophied and showed a round-shaped morphology (Figures 4C, D, arrowheads). However, in wild-type mice, OPN immunoreactivity was weak and showed a spindle-shaped morphology (Figures 4A, B).

From 4 weeks old on, in twy mice, OPN immunoreactivity was detected in cells in the spinal ligament (Figure 3B, arrows) and chondrogenic cells in the outer layer of the anulus fibrosus (Figure 3B, arrowheads), which was consistent with the expression pattern of OPN mRNA by *in situ* hybridization analysis. These trends were also seen in wild-type mice; however, OPN immunoreactivity was weak compared with that of twy mice (data not shown).

Analysis of OPN and COL10A1 mRNA by Northern Blot

At 2 week's old, considerable amounts of OPN transcripts were detected in all genotypes and there was no significant difference in the expression level among genotypes. At 16 weeks, robust expression of OPN mRNA was still detected in twy mice; however, it was reduced in the heterozygote and further reduced in wild-type mice (Figure 5).

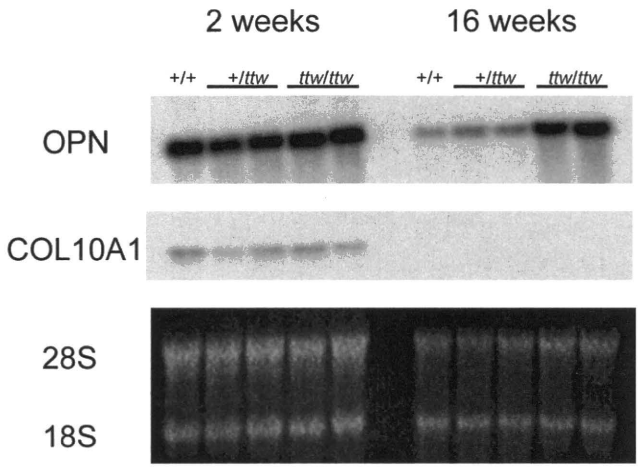

Figure 5. Temporal expression of OPN and COL10A1 mRNA in the cervicothoracic spine of wild-type, heterozygote (+/*ttw*), and twy mice (*ttw/ttw*) during growth. Twenty μg of total RNA from each sample was analyzed to quantify the levels of OPN and COL10A1 transcripts. At 2 weeks old, considerable amounts of OPN transcripts were detected in all genotypes with no significant difference in expression levels among them, while small amounts of COL10A1 transcripts were seen in all genotypes. At 16 weeks old, robust expression of OPN mRNA was still detected in twy mice, but no longer detected in the heterozygote or wild-type mice. Note that COL10A1 transcripts were hardly detected regardless of the genotype. Eighteen S and 28S served an internal standard for the amount and integrity of RNA preparation. Representative autographic images are shown.

To determine the ossification pattern for the spinal ligament of twy mice, we also investigated the temporal expression of the COL10A1 gene, an established marker for chondrocyte hypertrophy, during growth. At 2 weeks old, a small amount of COL10A1 transcripts was detected in all genotypes, with no significant differences noted among genotypes. Strikingly, at 16 weeks old, COL10A1 transcripts were hardly detected regardless of the genotype (Figure 5).

■ Discussion

The spinal lesion of the twy mouse is characterized by ectopic calcification that occurs in the outer layer of the anulus fibrosus from 4 weeks old and bony bridging over vertebral bodies that begins at 11 weeks old.[4] Histologic analyses using nondecalcified spinal tissues of twy mice showed intramembranous bone formation at the enthesis of the spinal ligament.[4,6] However, the present study using decalcified tissues demonstrated endochondral bone formation at the enthesis. Thus, ossification patterns for the spinal ligament of the twy mouse have been unknown to date.

In the spine of the twy mouse, OPN was detected in hypertrophic chondrocytes of the vertebral end plate, cells in the outer layer of the anulus fibrosus, cells in the spinal ligament, and osteoblasts in the primary spongiosa of the vertebral body. Of interest, from 4 weeks old on, expression of OPN in the twy mouse was enhanced in chondrogenic cells in the outer layer of the anulus fibrosus and cells in the spinal ligament, compared with age-matched wild-type mice. In particular, extracellular matrix around cells in the outer layer of the anulus fibrosus showed metachromasia with TB staining, suggesting that those cells possessed a chondrogenic phenotype. Furthermore, regions adjacent to the TB-stained area showed eosinophilia with HE staining, indicating that osteoid, immature bone is also formed there. Considering our previous study demonstrating localization of type II, IV, and XI collagen in the outer layer of the anulus fibrosus,[7] ossification of the spinal ligament in the twy mouse might be induced, at least in part, by endochondral ossification.

To determine whether ossification of the spinal ligament is mediated by endochondral bone formation, we extracted total RNA from the spine and investigated mRNA expression for OPN and COL10A1 at 2- and 16-week-old. During endochondral ossification, COL10A1 and OPN are expressed in hypertrophic chondrocytes. Although COL10A1 is specifically expressed in cells of chondrogenic lineage, OPN is expressed in cells of both chondrogenic and osteoblastic lineages.[21,22,24] At 2 weeks old, an equivalent amount of COL10A1 transcripts was detected in all genotypes. However, at 16 weeks old, COL10A1 transcripts were hardly detected regardless of genotype despite elevated levels of OPN seen in the twy mouse. These suggest that the major ossification process for the spinal ligament of twy mice is not canonical endochondral bone formation. At this point, in twy mice, a considerable amount of OPN was expressed in fibroblastic cells in hypertrophied spinal ligament rather than in hypertrophic chondrocytes in the anulus fibrosus. This also suggests that spinal hyperostosis of the twy mouse develops largely by ectopic ossification of the spinal ligament, but does not involve chondrocytes of vertebral disc-mediated endochondral ossification.

OPN, an extracellular matrix protein known to be important in cellular attachment, is also a useful marker for calcification during both intramembranous and endochondral ossification.[22–24] During fracture healing, expression of OPN is detected in osteocytes and osteoprogenitor cells in the subperiosteal callus,[27] but little OPN signal is seen in cuboidal osteoblasts.[25,27] Furthermore, OPN is preferentially expressed in late hypertrophic chondrocytes, but not in proliferating chondrocytes, and early hypertrophic chondrocytes in cartilaginous calluses.[22,24] Although OPN function in bone and cartilage metabolism remains to be elucidated, these observations suggest that OPN functions as a marker for calcification *in vivo*.

Overexpression of OPN in the spinal hyperostosis of the twy mouse seems understandable from the view point that OPN is a marker for calcification *in vivo*. Indeed, there have been many reports that OPN mRNA was overexpressed in pathologic lesions associated with ectopic calcification,[28–31] indicating that OPN may have a positive role in promoting calcification *in vivo*. OPN possesses the ability to bind significant amounts of Ca^{2+} through its electronegative glutamic and aspartic acid residues, serine/threonine kinase substrate sites, and putative calcium-binding mo-

tifs.[32] These properties of OPN likely contribute to ectopic calcification. However, the contribution of enhanced OPN expression to spinal hyperostosis seems to be paradoxical from the view point that OPN is an inhibitor of calcification. Why is spinal hyperostosis developed in the twy mouse despite local overexpression of OPN?

Previous *in vitro* and *in vivo* studies suggest that OPN not only inhibits mineral deposition, but also actively promotes its dissolution by physically blocking hydroxyapatite crystal growth and inducing expression of carbonic anhydrase II in monocytic cells, which promotes acidification of the extracellular milieu.[29] These findings indicate that recruitment of macrophages and/or monocytic cells and their bone-resorbing functions are important for OPN to regulate ectopic calcification. In other words, under abnormal ectopic ossification associated with overexpression of OPN, it should be considered that there might be some problems in OPN function.

Recently, it has emerged that OPN-knock-out mice are susceptible to ectopic calcification *in vivo*,[29,31] indicating that physiologic concentrations of OPN inhibit calcification. To the best of our knowledge, however, there have been no studies demonstrating the effects of an excessive amount of OPN on ectopic calcification *in vivo*. To explain spinal hyperostosis in the twy mouse associated with local overexpression of OPN, we think the possibility that overexpressed OPN in the spinal ligament does not fully exert its primary function as an inhibitor of calcification. Because it has been reported that phosphorylation of OPN is crucial for its anticarcific effects,[17,19,31] further studies will be necessary to verify whether OPN overexpressed in the twy mouse is functional (*i.e.*, phosphorylated).

In conclusion, the results presented here clearly establish overexpression of OPN in spinal hyperostosis of the twy mouse, and this hyperostosis was induced by ectopic ossification of the spinal ligament. Targeting OPN as a prime candidate molecule for inhibition of ectopic calcification may provide new therapeutic clues for hyperostotic diseases of the spine.

■ Key Points

- To verify the involvement of OPN in spinal hyperostosis in the twy mouse, a model for human OPLL, gene expression, and protein localization of OPN was analyzed by means of *in situ* hybridization, immunohistochemistry, and Northern blot analysis.
- OPN was overexpressed in hyperostotic spinal lesions of the twy mouse, and the hyperostosis was induced mainly by ectopic ossification of the spinal ligament.
- Because OPN is considered to be an inhibitor of calcification, further studies will be necessary to verify whether OPN overexpressed in the twy mouse is functional.

References

1. Hosoda Y, Yoshimura Y, Higaki S. Anew breed of mouse showing multiple osteochondral lesions: twy mouse [in Japanese]. *Ryumachi* 1981;21(suppl): 157–64.
2. Okawa A, Nakamura I, Goto S, et al. Mutation in *Npps* in a mouse model of ossification of the posterior longitudinal ligament of the spine. *Nat Genet* 1998;19:271–3.
3. Goto S, Yamazaki M. Pathogenesis of ossification of the spinal ligaments. In: Yonenobu K, Sakou T, Ono K, eds. *Ossification of the Posterior Longitudinal Ligament*. Tokyo, Japan: Springer-Verlag; 1997:29–37.
4. Tannno T. Experimental study on the spinal lesions in hyperostotic mouse (twy/twy): special reference to the pathogenesis of the spinal ligaments and to the action of ethane-1, 1-diphosphonate (EHDP) [in Japanese]. *J Jpn Orthop Assoc* 1992;66:1073–82.
5. Okawa A, Goto S, Moriya H. Calcitonin simultaneously regulates both periosteal hyperostosis and trabecular osteopenia in the spinal hyperostotic mouse (twy/twy) in vivo. *Calcif Tissue Int* 1999;64:239–47.
6. Terakado A, Tagawa M, Goto S, et al. Elevation of alkaline phosphatase activity induced by parathyroid hormone in osteoblast-like cells from the spinal hyperostotic mouse TWY (twy/twy). *Calcif Tissue Int* 1995;56:135–9.
7. Yamazaki M, Moriya H, Goto S, et al. Increased type IX collagen expression in the spinal hyperostotic mouse (twy/twy). *Calcif Tissue Int* 1991;48:182–9.
8. Forestier J, Lagier R. Ankylosing hyperostosis of the spine. *Clin Orthop* 1971;74:65–83.
9. Resnick D, Shaul SR, Robins JM. Diffuse idiopathic skeletal hyperostosis (DISH): Forestier's disease with extraspinal manifestations. *Radiology* 1975; 115:513–24.
10. Caswell AM, Ali SY, Russell RG. Nucleotide triphosphate pyrophosphatase of rabbit matrix vesicles, a mechanism for the generation of inorganic pyrophosphate in epiphyseal cartilage. *Biochim Biophys Acta* 1987;924:276–83.
11. Caswell AM, Russell RG. Evidence that ecto-nucleoside-triphosphate pyrophosphatase serves in the generation of extracellular inorganic pyrophosphate in human bone and articular cartilage. *Biochim Biophys Acta* 1988; 966:310–7.
12. Huang R. Expression of the murine plasma cell nucleotide pyrophosphohydrolase PC-1 is shared by human liver, bone, and cartilage cells: regulation of PC-1 expression in osteosarcoma cells by transforming growth factor-beta. *J Clin Invest* 1994;94:560–7.
13. Fleisch H. Diphosphonates: history and mechanisms of action. *Metab Bone Dis Relat Res* 1981;3:279–88.
14. Oldberg A, Franzen A, Heinegard D. Cloning and sequence analysis of rat bone sialoprotein (osteopontin) cDNA reveals an Arg-Gly-Asp cell-binding sequence. *Proc Natl Acad Sci USA* 1986;83:8819–23.
15. Miyauchi A, Alvarez J, Greenfield EM. Recognition of osteopontin and related peptides by an (alpha v beta 3) integrin stimulates immediate cells signals in osteoclasts. *J Biol Chem* 1991;266:20369–74.
16. Giachelli CM, Schwartz SM, Liaw L. Molecular and cellular biology of osteopontin. *Trends Cardiovasc Med* 1995;5:88–95.
17. Hunter GK, Kyle CL, Goldberg HA. Modulation of crystal formation by bone phosphoproteins: structural specificity of the osteopontin-mediated inhibition of hydroxyapatite formation. *Biochem J* 1994;300:723–8.
18. Boskey AL, Maresca M, Ullrich W, et al. Osteopontin-hydroxyapatite interactions in vitro: inhibition of hydroxyapatite formation and growth in a gelatin-gel. *Bone Miner* 1993;22:147–59.
19. Jono S, Peinado C, Giachelli CM. Phosphorylation of osteopontin is required for inhibition of vascular smooth muscle cell calcification. *J Biol Chem* 2000; 275:20197–203.
20. Groski JP. Acidic phosphoproteins from bone matrix: a structural rationalization of their role in biomineralization. *Calcif Tissue Int* 1992;50:391–6.
21. Nakajima F, Ogasawara A, Goto K, et al. Spatial and temporal gene expression in chondrogenesis during fracture healing and the effects of basic fibroblast growth factor. *J Orthop Res* 2001;19:935–44.
22. Nakazawa T, Nakajima A, Shiomi K, et al. Effects of low-dose, intermittent treatment with recombinant human parathyroid hormone (1–34) on chondrogenesis in a model of experimental fracture healing. *Bone* 2005; 37:711–9.
23. Nakajima F, Nakajima A, Ogasawara A, et al. Effects of a single percutaneous injection of basic fibroblast growth factor on the healing of a closed femoral shaft fracture in the rat. *Calcif Tissue Int* 2007;81:132–8.
24. Ogasawara A, Nakajima A, Nakajima F, et al. Molecular basis for affected cartilage formation and bone union in fracture healing of the streptozotocin-induced diabetic rat. *Bone* 2008;43:832–9.
25. Yamazaki M, Majeska RJ, Yoshioka H, et al. Spatial and temporal expression of fibril-forming minor collagen genes (Type V and XI) during fracture healing. *J Orthop Res* 1997;15:757–64.

26. Hashimoto M, Koda M, Ino H, et al. Upregulation of osteopontin in rat spinal cord microglia after traumatic injury. *J Neurotrauma* 2003;20:287–96.
27. Hirakawa K, Hirota S, Ikeda T, et al. Localization of the mRNA for bone matrix proteins during fracture healing as determined by in situ hybridization. *J Bone Miner Res* 1994;9:1551–7.
28. Ikeda T, Shirasawa T, Esaki Y, et al. Osteopontin mRNA is expressed by smooth muscle-derived form cells in human atherosclerotic lesions of the aorta. *J Clin Invest* 1993;92:2814–20.
29. Steitz SA, Speer MY, McKee MD, et al. Osteopontin inhibits mineral deposition and promotes regression of ectopic calcification. *Am J Pathol* 2002;161:2035–46.
30. Harmey D, Hessle L, Narisawa S, et al. Concerted regulation of inorganic pyrophosphate and osteopontin by Akp2, Enpp1, and Ank: an integrated model of the pathogenesis of mineralization disorders. *Am J Pathol* 2004; 164:1199–209.
31. Ohri R, Tung E, Rajachar R, et al. Mitigation of ectopic calcification in osteopontin-deficient mice by exogenous osteopontin. *Calcif Tissue Int* 2005;76:307–15.
32. Chen Y, Bal BS, Groski JP. Calcium and collagen binding properties of osteopontin, bone sialoprotein, and bone acidic glycoprotein-75 from bone. *J Biol Chem* 1992;276:24871–8.

A microRNA regulatory mechanism of osteoblast differentiation

Hiroyuki Inose[a], Hiroki Ochi[b], Ayako Kimura[a,c], Koji Fujita[a,c], Ren Xu[a], Shingo Sato[a], Makiko Iwasaki[a], Satoko Sunamura[d], Yasuhiro Takeuchi[e], Seiji Fukumoto[f], Kuniaki Saito[g], Takashi Nakamura[h], Haruhiko Siomi[g], Hiroshi Ito[d], Yoshiyasu Arai[a], Ken-ichi Shinomiya[a,c], and Shu Takeda[a,d,1]

[a]Department of Orthopedics, Graduate School, [c]Global Center of Excellence Program, and [h]Department of Developmental and Regenerative Biology, Tokyo Medical and Dental University, 1-5-45 Yushima, Bunkyo-ku, Tokyo 113-8519, Japan; [b]Department of Veterinary Science, Faculty of Veterinary Medicine, Nippon Veterinary and Life Science University, 1-7-1 Kyonan-cho, Musashino-shi, Tokyo 180-8602, Japan; [e]Toranomon Hospital Endocrine Center, 2-2-2 Toranomon, Minato-ku, Tokyo 105-8470, Japan; [f]Division of Nephrology and Endocrinology, Department of Internal Medicine, University of Tokyo Hospital, 7-3-1 Hongo, Bunkyo-ku, Tokyo 113-8655, Japan; and [d]Section of Nephrology, Endocrinology and Metabolism, Department of Internal Medicine and [g]Department of Molecular Biology, Keio University School of Medicine, 35 Shinanomachi, Shinjuku-ku, Tokyo 160-8582, Japan

Edited by Clifford J. Tabin, Harvard Medical School, Boston, MA, and approved October 13, 2009 (received for review August 17, 2009)

Growing evidence shows that microRNAs (miRNAs) regulate various developmental and homeostatic events in vertebrates and invertebrates. Osteoblast differentiation is a key step in proper skeletal development and acquisition of bone mass; however, the physiological role of non-coding small RNAs, especially miRNAs, in osteoblast differentiation remains elusive. Here, through comprehensive analysis of miRNAs expression during osteoblast differentiation, we show that miR-206, previously viewed as a muscle-specific miRNA, is a key regulator of this process. miR-206 was expressed in osteoblasts, and its expression decreased over the course of osteoblast differentiation. Overexpression of miR-206 in osteoblasts inhibited their differentiation, and conversely, knockdown of miR-206 expression promoted osteoblast differentiation. In silico analysis and molecular experiments revealed connexin 43 (Cx43), a major gap junction protein in osteoblasts, as a target of miR-206, and restoration of Cx43 expression in miR-206-expressing osteoblasts rescued them from the inhibitory effect of miR-206 on osteoblast differentiation. Finally, transgenic mice expressing miR-206 in osteoblasts developed a low bone mass phenotype due to impaired osteoblast differentiation. Our data show that miRNA is a regulator of osteoblast differentiation.

Connexin43 | miR-206 |

The osteoblast, a cell type of a mesenchymal origin, plays a major role in skeletal development and bone formation (1, 2). Understanding the regulatory mechanism of osteoblast differentiation is a prerequisite for developing strategies to treat bone loss diseases such as osteoporosis (3–5). In the last two decades, progress in molecular and genetic research has uncovered various regulatory processes of osteoblast differentiation (1, 2, 4). Central to this regulation are transcription factors; Runx2, Osterix, and β-catenin are, to date, the transcription factors known to be essential for osteoblast differentiation (2). In addition, while some transcription factors, including C/EBPβ, Smad1, and Smad5, bind to Runx2 and enhance its transcriptional activity, others, such as Twist, inhibit Runx2 transcriptional activity (6). However, given the fact that the number of coding genes in vertebrates and invertebrates (which lack a skeleton) is comparable (7), there must be additional mechanisms for controlling skeletal development other than transcriptional regulation of gene expression.

Recently, miRNAs have emerged as important regulators in various developmental, physiological, and pathological conditions such as tumorigenesis, viral infection, and cell differentiation and function (8–10). miRNAs are single-stranded small RNA molecules that are approximately 21 or 22 nucleotides long (9). They do not encode protein; instead, they regulate the level of other proteins by decreasing messenger RNA (mRNA) levels or inhibiting translation by binding the 3′UTR of the target mRNA (8). Surprisingly, non-coding RNA accounts for 98% of all genomic output in humans (11), and it has been proposed that the proportion of non-coding RNA to protein-coding RNA is correlated with developmental complexity (12).

Previous reports implicated miRNAs in the differentiation of osteoclasts and osteoblasts (13–21). However, their importance in the regulation of osteoblast differentiation in vivo, if any, remains to be established. Here we show that one particular miRNA, miR-206, is expressed in the osteoblastic cell lineage and that its expression gradually decreases in parallel with osteoblast differentiation. Interestingly, modulating miR-206 expression in osteoblasts markedly affects their differentiation potential in part by altering the accumulation of connexin 43 (Cx43). Finally, osteoblast-specific expression of miR-206 in vivo leads to severe bone loss due to impairment of osteoblast differentiation. Thus, this study reveals a physiological regulatory mechanism of osteoblast differentiation mediated by miRNA.

Results

Identification of miRNAs Whose Expression Varies During Osteoblast Differentiation. To study the potential involvement of miRNAs in osteoblast differentiation, we first attempted to identify miRNAs that are expressed in the osteoblastic cell lineage, particularly miRNAs whose expression is altered during osteoblast differentiation. To that end, we treated multipotent C2C12 mesenchymal progenitor cells with recombinant BMP-2 for 2 days, an established model for studying osteoblast differentiation (22). We then comprehensively analyzed the expression of miRNAs before and after BMP-2 treatment using a microarray that detects all known miRNAs (23). miR-133a was downregulated by BMP-2 treatment (Fig. 1*A* and Figs. S1 and S2*A*) as previously reported (13), suggesting that the experiment was properly conducted. Osteoblasts express many miRNAs, and most of the miRNAs (36%) were downregulated by BMP-2 treatment, while only 4% of them were upregulated (Fig. 1*A* and Fig. S1). Of these, we were interested in miR-206 because its expression was most significantly downregulated during osteoblast differentiation (Fig. 1*A*). As miR-206 was originally shown to be expressed exclusively in skeletal muscle and heart (24–28), we first verified its expression in the osteoblastic lineage using primary mouse osteoblasts and bones by four different experiments. First, as

Author contributions: Y.T., S.F., T.N., H.S., H. Ito, Y.A., K. Shinomiya, and S.T. designed research; H. Inose, H.O., A.K., K.F., R.X., S. Sato, M.I., S. Sunamura, and K. Saito performed research; H. Inose and S.T. analyzed data; and S.T. wrote the paper.

The authors declare no conflict of interest.

This article is a PNAS Direct Submission.

[1]To whom correspondence should be addressed. E-mail: shu-tky@umin.ac.jp.

This article contains supporting information online at www.pnas.org/cgi/content/full/0909311106/DCSupplemental.

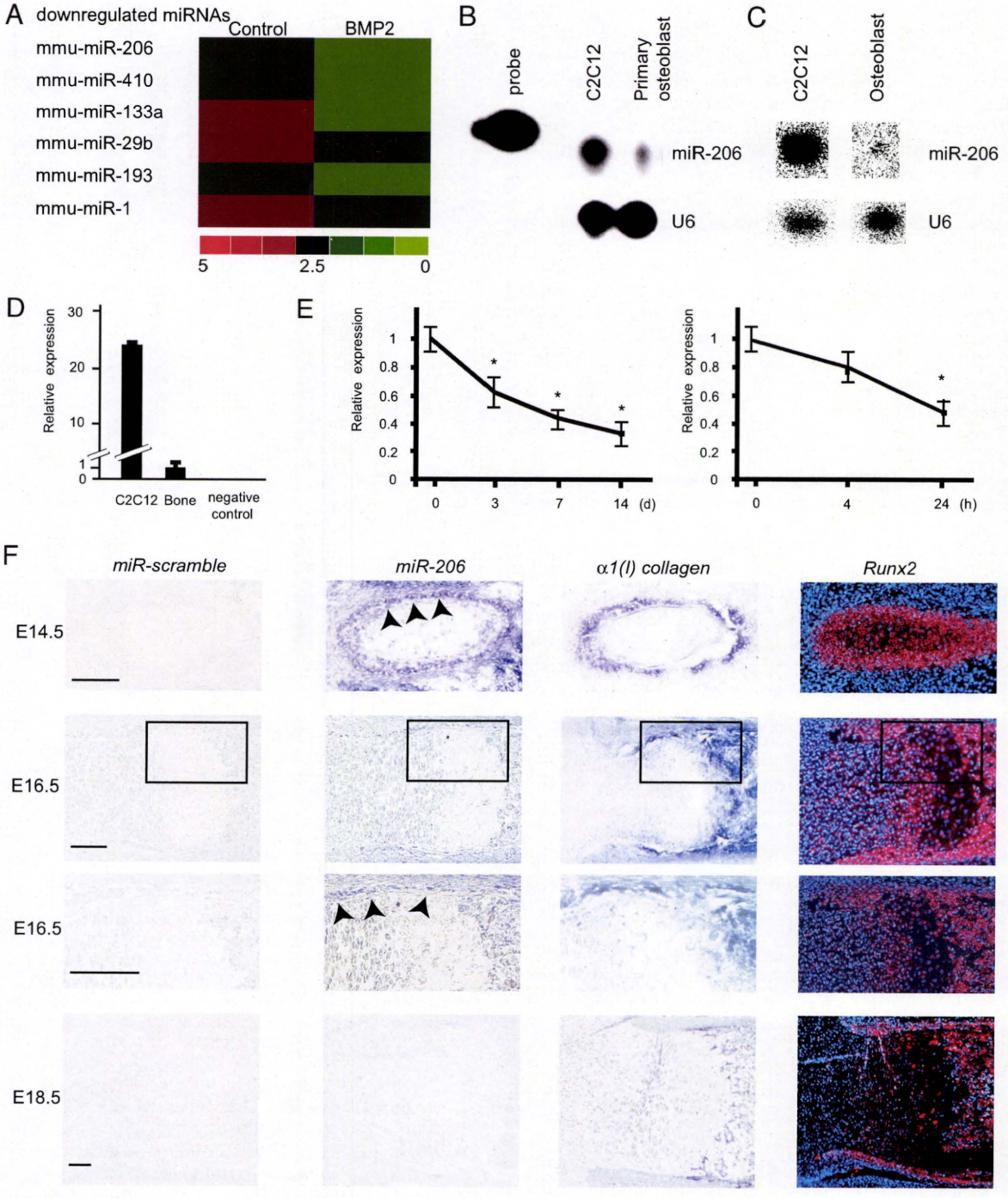

Fig. 1. Expression of miR-206 during osteoblast differentiation. (*A*) miRNA array expression data from C2C12 cells cultured in growth medium (Control) or in differentiation medium containing BMP-2. Red denotes high expression and green denotes low expression relative to the median; only the representative miRNA nodes that were significantly downregulated in the differentiation medium are shown. (*B–D*) Expression of miR-206 in osteoblasts: RNase protection assay (*B*), Northern blot analysis (*C*), and quantitative RT-PCR analysis (*D*) to detect miR-206 expression in osteoblasts. Total RNA was isolated from primary mouse osteoblasts, mouse femur or C2C12 cells. U6 RNA was used as a loading control. Note the distinct expression of miR-206 in primary osteoblasts and bone (*B–D*). (*E*) Change in miR-206 expression during osteoblast differentiation: quantitative RT-PCR analysis. Mouse primary osteoblasts were treated in differentiation medium (*Left*) or with the addition of BMP-2 (*Right*) for each indicated length of time. Note the significant decrease in parallel with the progression of osteoblast differentiation. *, $P < 0.05$ vs. 0 time point, $n = 6$. (*F*) In situ hybridization analysis of miR-206 expression in mouse embryos: Rib (E14.5, *Top*) and femur (E16.5, middle and E18.5, *Bottom*) cryosections. Bottom panel of E16.5 embryo shows the higher magnification of the black rectangular region in the top panel. Adjacent sections were hybridized with *scramble-miRNA* (left), *miR-206* (*Middle Left*), *α1(I) collagen* (*Middle Right*), and *Runx2* (*Right*) probes. Note the miR-206 expression in perichondrium osteoblastic cells at E14.5 (arrowheads) and in cells of bone collar at E16.5 (arrowheads). (Scale bar, 100 μm.)

shown by an RNase protection assay, miR-206 was clearly expressed in primary osteoblasts (Fig. 1*B*). Second, by Northern blot analysis, which is almost 10 times less sensitive than an RNase protection assay (29, 30), miR-206 was also shown to be expressed in primary osteoblasts (Fig. 1*C*). Third, by real-time PCR analysis specific to miR-206, we observed miR-206 expres-

sion both in femur and primary osteoblasts (Fig. 1 *D* and *E*), and interestingly, miR-206 expression gradually decreased during the course of osteoblast differentiation (Fig. 1*E*). Fourth and most importantly, to investigate the dynamic pattern of miR-206 expression in bone, we performed in situ hybridization analysis using DIG-labeled probes. At E14.5, miR-206 was expressed in muscle and perichondrium osteoblastic cells, whose identity was verified by the coexpression of *α1(I) collagen* and *Runx2*, markers for osteoblasts (Fig. 1*F*). At E16.5, miR-206 was still expressed in the cells of the bone collar, although the expression was decreased compared to the expression at E14.5 (Fig. 1*F*). At E18.5, miR-206 expression in bone was close to background level (Fig. 1*F*). The gradual decrease of miR-206 expression during skeletogenesis in vivo is consistent with its gradual decrease of expression during the course of in vitro osteoblast differentiation. To further confirm in vivo expression of miR-206 in osteoblasts, we also performed double staining for in situ hybridization to detect miR-206 and immunohistochemistry to detect Runx2. High resolution confocal microscopic analysis revealed that miR-206 colocalize with Runx2 in osteoblast (Fig. S3). Taken together, these four independent experiments confirmed that miR-206 is expressed in the osteoblastic cell lineage.

miR-206 Regulates Osteoblast Differentiation. The decrease in the expression of miR-206 during osteoblast differentiation prompted us to test if miR-206 inhibits osteoblast differentiation. To this end, we infected a vector expressing both miR-206 and a blasticidin-resistance gene into C2C12 cells and isolated five stable blasticidin-resistant clones that also express miR-206 to determine if continuous expression of miR-206 affected their ability to differentiate into osteoblasts. As controls, we also infected either an empty vector or a miR-133-expressing vector. C2C12 cells expressing empty vector differentiated normally into the osteoblastic lineage upon BMP-2 treatment. In contrast, osteoblastic differentiation of C2C12 cells expressing miR-133 was significantly impaired (Fig. S2*B*), as previously reported. Importantly, none of the five clones expressing miR-206 differentiated into the osteoblastic lineage, as shown by the lack of induction of alkaline phosphatase activity (Fig. 2*A*). To rule out the possibility that stable expression of miR-206 altered the properties of C2C12 cells, we also transiently transfected a miR-206-expressing vector into C2C12 cells. In this transient DNA transfection assay, miR-206 also repressed osteoblastic differentiation (Fig. 2*B*). To test if miR-206 regulates osteoblast differentiation in a physiological manner, we next used primary mouse osteoblasts because C2C12 is a myogenic cell line. The results showed that continuous expression of miR-206 significantly inhibited osteoblast differentiation as demonstrated by the decrease in alkaline phosphatase activity and *bglap* expression (Fig. 2*C* and Fig. S4). Interestingly, miR-206 expression did not affect Runx2 mRNA expression, indicating that miR-206 regulates osteoblast differentiation independently of Runx2 (Fig. 2*C*).

Because it has been shown that expression of miR-206 induces myogenic differentiation (24, 27, 28), we asked whether miR-206 expression induces myogenic transdifferentiation of osteoblasts; however, no expression of myogenic genes such as *MyoD* or *Myf5* (31) was detected, indicating that miR-206 does not induce myogenic differentiation (Fig. 2*C*)

Since overexpression of miR-206 inhibits osteoblast differentiation, we next asked whether decreasing miR-206 expression would accelerate their differentiation. Indeed, knockdown of miR-206 significantly induced osteoblast differentiation (Fig. 2*D*). Taken together, these results demonstrate that miR-206, which is expressed in the osteoblastic cell lineage, physiologically regulates osteoblast differentiation.

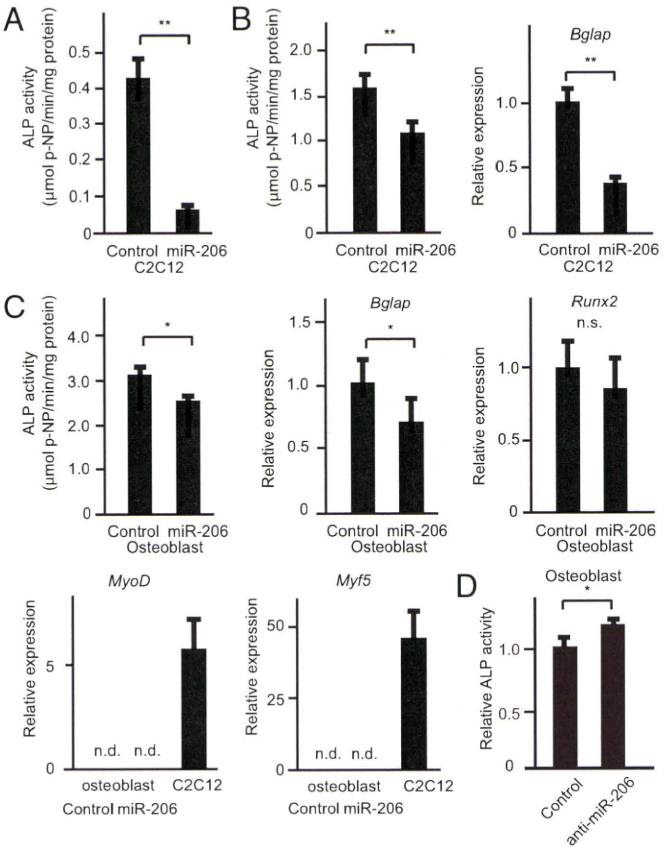

Fig. 2. Regulation of osteoblast differentiation by miR-206. (*A* and *B*) Effect of miR-206 expression on BMP-2-dependent C2C12 cell differentiation: C2C12 cells constitutively expressing miR-206 (*A*) or transiently transfected with miR-206 (*B*). Alkaline phosphatase activity (*A* and *B*, *Left*) and *bglap* gene expression (*B*, *Right*) were analyzed. Note the decreased osteoblastic differentiation in miR-206 expressing cells. **, $P < 0.01$, $n = 6–8$. (*C*) Effect of miR-206 continuous expression on primary mouse osteoblast differentiation: primary mouse osteoblasts infected with pAd-miR-206 or control adenovirus were cultured. Subsequently, alkaline phosphatase activity assay (*Top Left*) and quantative RT-PCR analysis for the indicated genes were analyzed. GAPDH was used as an internal control. n.s., not significant. n.d., not detected. *, $P < 0.05$, $n = 6–8$. (*D*) Effect of miR-206 knockdown on osteoblast differentiation: osteoblasts were transfected with a miR-206 inhibitor or control. Subsequently, alkaline phosphatase activity was analyzed. Note the significant increase by the miR-206 inhibitor. *, $P < 0.05$, $n = 6$.

Connexin 43 Is One Molecular Target of miR-206 in Osteoblasts. We next studied the molecular mechanism by which miR-206 inhibits osteoblast differentiation. To identify target genes of miR-206, we relied on a computational approach using two different established databases (32, 33). Among the many genes that were predicted to be potential targets by both databases, we focused on Cx43, a gap junction protein expressed in osteoblasts that plays a major role in osteoblast differentiation and function; indeed, Cx43-deficient mice display low bone mass due to osteoblast dysfunction (34, 35). Two putative target sequences for miR-206 were found in the 3′UTR region of Cx43 (Fig. 3*A*). At first, we tested if miR-206 regulated Cx43 expression using a reporter plasmid in which the two putative binding sites of the Cx43 3′UTR were cloned into the 3′UTR of the luciferase gene (Fig. 3*B*). As expected from in silico analysis, ectopic expression of miR-206 significantly decreased luciferase activity (Fig. 3*B*); furthermore, ectopic expression of miR-206 downregulated endogenous Cx43 protein expression without affecting *Cx43* mRNA expression (Fig. 3*C*). Taken together, these results identify Cx43 as a bona fide target of miR-206 in vivo.

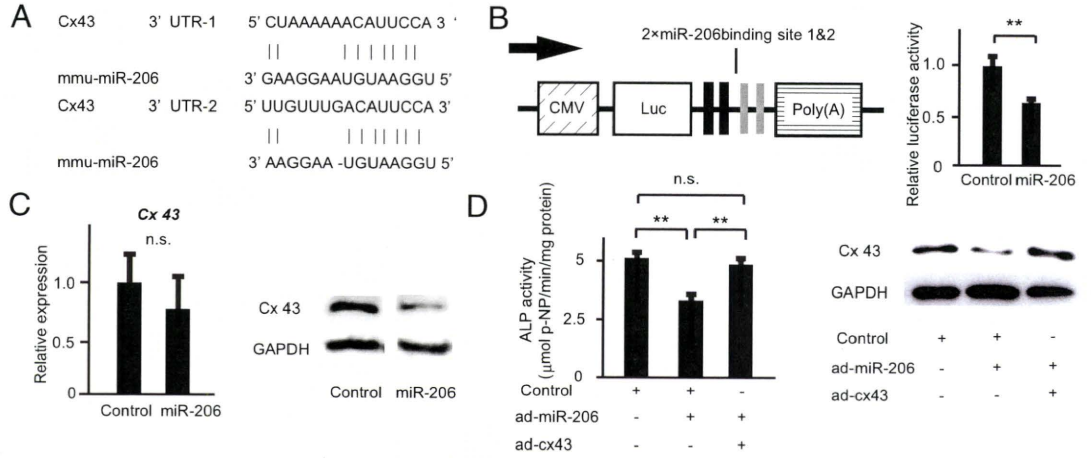

Fig. 3. Identification of miR-206 target genes in osteoblast differentiation. (*A*) Alignment of miR-206 showing complementary pairing to the Cx43 3′ UTR. (*B*) Schematic presentation of the reporter plasmid used to analyze the effect of the Cx43 3′ UTR on luciferase activity (*Left*). Effect of miR-206 expression on a luciferase reporter plasmid carrying the Cx43 3′ UTR was analyzed (*Right*). Cells were transfected with either the miR-206 expression plasmid or a control. The ratio of reporter (firefly) to control (renilla) was plotted. CMV: cytomegalovirus promoter, Luc: luciferase. **, $P < 0.01$, $n = 6$. (*C*) miR-206 targets Cx43 and regulates its expression. Cells were transfected with the miR-206 expression plasmid or a control. Quantitative RT-PCR analysis (*Left*) and Western blot analysis for Cx43 (*Right*) were subsequently performed. GAPDH was used as an internal control. n.s., not significant; $n = 6–8$. (*D*) Cx43 rescues the inhibitory effect of miR-206 on osteoblast differentiation. Primary osteoblasts expressing miR-206 were infected with either the Cx43-expressing virus (pAd-Cx43) or control adenovirus. Subsequently, alkaline phosphatase activity was analyzed. Note that the inhibitory effect of miR-206 on osteoblast differentiation was reversed by co-expression of Cx43. (*Left*, alkaline phosphatase activity; *Right*, Western blot) **, $P < 0.01$, $n = 6$.

To address if Cx43 is a physiologically important target of miR-206 during osteoblast differentiation, we asked whether restoring Cx43 expression rescued the impairment of osteoblast differentiation caused by continuous miR-206 expression. Continuous expression of miR-206 in osteoblasts decreased osteoblast differentiation and Cx43 protein expression (Fig. 3*C*). However, when we co-expressed Cx43 together with miR-206, the inhibitory effect of miR-206 on osteoblast differentiation was markedly rescued (Fig. 3*D*). Importantly, the expression level of Cx43 protein was similar between control cells and cells co-expressing both miR-206 and Cx43, which indicates that restoration of Cx43 protein expression is sufficient to obtain normal osteoblast differentiation in miR-206-expressing osteoblasts (Fig. 3*D*).

miR-206 Is a Regulator of Bone Formation in Vivo. Lastly, to address the in vivo role of miR-206 in bone formation, we generated transgenic (tg) mice specifically expressing miR-206 in osteoblasts using the *α1(I) collagen* promoter (Fig. 4*A* and Fig. S5). α1(I) miR-206 tg mice displayed a low bone mass phenotype both in trabecular and cortical bones by μCT analysis and histology (Fig. 4 *A* and *B*). Furthermore, bone histomorphometric analysis revealed that the bone formation rate, an indicator of osteoblast function, was significantly decreased in α1(I) miR-206 mice (Fig. 4 *B* and *C*). In contrast, osteoclast surface, a marker of bone resorption, was similar in wild-type mice and α1(I) miR-206 tg mice, indicating that osteoclastic bone resorption was not affected (Fig. 4*C*). The expression of osteoblastic marker genes such as *Akp2* was significantly downregulated in α1(I) miR-206 tg mice (Fig. 4*D*). Importantly, Cx43 protein expression was significantly reduced in α1(I) miR-206 tg mice, while the expression of Runx2 and Osterix was not affected in these mice (Fig. 4 *D* and *E*), further indicating that miR-206 regulates osteoblast differentiation through Cx43 independently of Runx2 and Osterix. Of note, the lack of expression of myogenic marker genes in real-time PCR and the absence of Troponin I protein in immunohistochemistry (36) clearly demonstrated that there was no ectopic muscle differentiation in α1(I) miR-206 tg mice (Fig. 4 *B* and *D*). Collectively, overexpression of miR-206 in osteoblasts inhibited osteoblast differentiation, which led to low bone mass in vivo.

Discussion

We demonstrate here an inhibitory role of miR-206 during osteoblast differentiation. First, we showed that miR-206 is expressed in the osteoblastic lineage and that this expression gradually decreases during osteoblast differentiation. Then we demonstrated that modulating the expression of miR-206 in osteoblasts affects osteoblast differentiation and that one of the targets of miR-206 is Cx43. Finally, we showed that miR-206 regulates osteoblast differentiation in vivo. Recent reports suggested the involvement of miRNAs in osteoblast differentiation (13–20). However, these reports were based only on in vitro observations using a cell line. To our knowledge, this study demonstrates an in vivo regulatory role of miRNA in osteoblast differentiation.

It was previously shown that miR-206 induces myogenic differentiation (24, 27, 28). Therefore, we were concerned that the observed inhibitory effect of miR-206 in osteoblast differentiation was attributable only to an increase of differentiation into the myoblastic lineage, or alternatively, that miR-206 transdifferentiates osteoblasts into the myoblastic lineage. However, the experimental evidence argues against these hypotheses. Indeed, primary osteoblasts continuously expressing miR-206 do not express myogenic markers such as *MyoD* or *Myf5*. Furthermore, α1(I) miR-206 tg mice do not demonstrate any evidence of ectopic muscle differentiation in bone. Notably, the fact that to overexpress miR-206 we used the α1(I) collagen promoter, which is active only in cells committed to the osteoblastic lineage (37), and that these tg mice developed bone abnormalities strongly suggests that miR-206 directly affects osteoblast differentiation independently from any function it has during myogenic differentiation.

There was also another concern that miR-206 was expressed only in myogenic cells and inhibited osteoblastic genes in them. However, we observed that miR-206 was expressed in osteoblastic cells by four different experimental procedures. Moreover, the fact that the knockdown of miR-206 in osteoblasts

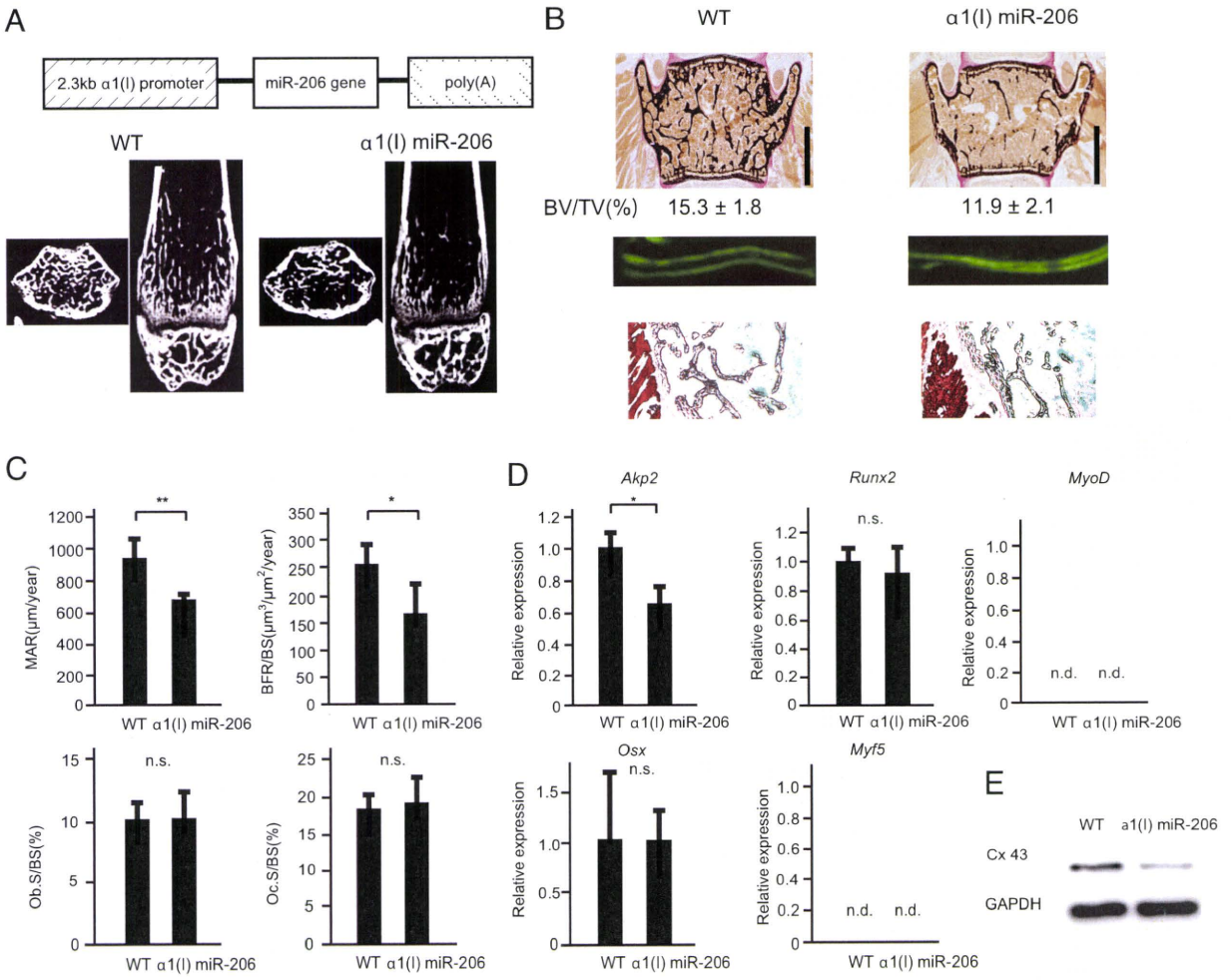

Fig. 4. Low bone mass in α1(I) miR-206 tg mice due to reduced bone formation. (*A*) Structure of the construct for osteoblast-specific α1(I) miR-206 tg mice (*Top*). μCT analysis of the femurs of 6-week-old female wild-type (WT) or α1(I) miR-206 tg mice (*Bottom*). Axial section (*Left*) and coronal section (*Right*). (*B*) Histological analysis of the vertebrae of 6-week-old female WT or α1(I) miR-206 tg mice. Von Kossa staining (*Top*). Bone volume per tissue volume (BV/TV). (Scale bars, 1 mm.) The distance between the two calcein labels represents the bone formation rate (middle). Note the significant decrease in bone formation in α1(I) miR-206 tg mice. Immunohistochemical staining for Troponin I (*Bottom*). Note the absence of Troponin I immunoreactivity (brown) in the vertebrae of α1(I) miR-206 tg mice in contrast to the intense staining in skeletal muscle. (*C*) Histomorphometric analysis of the vertebrae of 6-week-old female mice. Mineral apposition rate (MAR), bone formation rate over bone surface area (BFR/BS), osteoblast surface area over bone surface area (Ob.S/BS), osteoclast surface area over bone surface area (Oc.S/BS). n.s, not significant. *, $P < 0.05$, **, $P < 0.01$, $n = 6$–7. (*D*) Gene expression in α1(I) miR-206 tg mice. Quantitative RT-PCR analysis of osteoblastic genes (*Akp2*, *Runx2*, and *Osx*) and myogenic genes (*Myf5*, *MyoD*). Primary calvarial osteoblasts were isolated from WT or α1(I) miR-206 tg mice and used for subsequent analyses. n.s.: not significant. *, $P < 0.05$, $n = 6$. (*E*) Western blot analysis of calvaial bones of 2-week-old female mice. Note the decrease in Cx43 protein expression in α1(I) miR-206 tg mice.

accelerated their differentiation demonstrates that miR-206 is expressed in osteoblasts and plays a role in their differentiation.

Muscle-specific miRNAs comprise a well-defined family consisting of miR-1, miR-133, and miR-206. Interestingly, while miR-1 and −133 are expressed in *Drosophila* and vertebrates, miR-206 is not expressed in *Drosophila*. Instead, it is only expressed in vertebrates. This suggests that miR-206 evolved at a different period from miR-1 and miR-133 and thus may play a role other than the regulation of myogenic differentiation exhibited by miR-1 and miR-133.

Our observation that the inhibitory effect of miR-206 on osteoblast differentiation was rescued by the restoration of Cx43 suggests that Cx43 is a bona fide target of miR-206 in osteoblast differentiation. Indeed, while miR-206-expressing osteoblasts have a defect in osteoblast differentiation, they do not show any proliferative abnormality. This result is consistent with the normal proliferation of Cx43-deficient osteoblasts (34, 35). However, given that a miRNA can regulate multiple target genes (8), the effect of miR-206 may not depend solely on Cx43. Indeed, although osteoblast-specific Cx43-deficient mice have a normal mineral apposition rate (34), α1(I) miR-206 tg mice have a 30% decrease in the same parameter, suggesting the involvement of other molecules in miR-206-mediated bone formation defects.

Interestingly, parathyroid hormone (PTH), a well-known regulator of osteoblast differentiation, has been shown to regulate Cx43 expression through a posttranscriptional modification of Cx43 mRNA (38), and the anabolic response of PTH is attenuated in Cx43-deficient mice (34). Because miR-206 regulates both osteoblast differentiation and Cx43 mRNA stability, we tested whether PTH regulates Cx43 through a modification of miR-206 expression. However, PTH did not affect miR-206 expression.

It is interesting that miR-206 is strongly expressed in perichondrium, whereas its expression in trabecular bone is less (Fig. 1*F*). Considering that osteoblasts are derived from immature

osteoprogenitor cells located in the perichondrium (39), strong expression of miR-206 in the perichondrium suggests that miR-206 may work to keep osteoblast immature and decrease of miR-206 expression is important for proper osteoblastic differentiation, which is in agreement with our in vitro observations. Currently, the molecular mechanism accounting for the down-regulation of miR-206 expression during osteoblast differentiation is unknown. Because miR-206 is expressed in myogenic (24–28), adipocytic (40), and osteoblastic cells, all of mesenchymal origin, and miR-206 regulates both myogenic and osteoblastic differentiation, it is tempting to hypothesize that transcription factors involved in the differentiation of mesenchymal stem cells into specific cell lineages also regulate miR-206 expression. In this context, myogenic factors were shown to bind the upstream sequences of miR-206 (26). Therefore, it is possible that essential transcription factors for osteoblast differentiation, such as Runx2 and Osterix, also regulate miR-206 expression. Indeed, there are many putative binding sites for these factors in the sequence upstream of miR-206.

In conclusion, we demonstrated a regulatory role of miRNA in osteoblast differentiation in vivo. From a clinical point of view, inhibiting miRNA expression (41) may lead to therapies for bone degenerative diseases such as osteoporosis.

Materials and Methods

Cell Culture, Microarrays, Alkaline Phosphatase Assay, and Dual-Luciferase Reporter Assay. Primary osteoblast and C2C12 cells were cultured and alkaline phosphatase activity (Wako, LabAssay ALP) was measured as previously described (42). Microarray analysis was performed as previously described (23). The activities of luciferase were determined by the dual-luciferase reporter assay (Promega). Further details are provided in the *SI Text*.

Cloning and Gene Expression. Genomic fragments of miR-206 precursors were amplified by PCR. miRNA expression was detected by an RNase protection assay using a mirVANA miRNA kit (Ambion) or quantitative RT-PCR with Mx3000P (Stratagene). Northern blot analysis was performed as previously reported (43). 3′-UTR of Cx43 was subcloned into downstream of the luciferase gene for Cx43–3′-UTR reporter construction.

Western Blot Analysis, Immunohistochemistry, and in Situ Hybridization. Western blot analysis and immunohistochemistry were performed according to a standard protocol (42). In situ hybridization was performed using DIG labeled probe [miR-206, miR-scramble and α1(I) collagen] and ^{35}S-labeled riboprobe (Runx2) as reported in ref. 44 with modifications. Further details are provided in the *SI Text*.

Transgenic Mice, Histology, and Histomorphometry. The genomic fragment of the miR-206 precursor was cloned into a plasmid containing a 2.3-kb α1(I) collagen promoter and microinjected as described in ref. 37. We performed histomorphometric analysis using the Osteomeasure System (Osteometrics) as described in ref. 42. Further details are provided in the *SI Text*.

Statistics. All data are presented as means ± SE. ($n \geq 6$). We performed statistical analysis by Student's t test, and $P < 0.05$ was considered statistically significant.

ACKNOWLEDGMENTS. We thank Dr. Gerard Karsenty for discussion and Takako Usami for technical assistance. This work was supported by the Japan Society for the Promotion of Science grants (to Y.A., K.S., and S.T.) and Uehara Memorial Foundation grant (to S.T.).

1. Karsenty G, Kronenberg HM, Settembre C (2009) Genetic control of bone formation. *Annu Rev Cell Dev Biol* , in press.
2. Komori T (2006) Regulation of osteoblast differentiation by transcription factors. *J Cell Biochem* 99:1233–1239.
3. Khosla S, Westendorf JJ, Oursler MJ (2008) Building bone to reverse osteoporosis and repair fractures. *J Clin Invest* 118:421–428.
4. Rosen CJ (2005) Clinical practice. Postmenopausal osteoporosis. *N Engl J Med* 353:595–603.
5. Sambrook P, Cooper C (2006) Osteoporosis. *Lancet* 367:2010–2018.
6. Franceschi RT, Ge C, Xiao G, Roca H, Jiang D (2007) Transcriptional regulation of osteoblasts. *Ann N Y Acad Sci* 1116:196–207.
7. Venter JC, et al. (2001) The sequence of the human genome. *Science* 291:1304–1351.
8. Hobert O (2008) Gene regulation by transcription factors and microRNAs. *Science* 319:1785–1786.
9. Kloosterman WP, Plasterk RH (2006) The diverse functions of microRNAs in animal development and disease. *Dev Cell* 11:441–450.
10. Stefani G, Slack FJ (2008) Small non-coding RNAs in animal development. *Nat Rev Mol Cell Biol* 9:219–230.
11. Mattick JS (2001) Non-coding RNAs: The architects of eukaryotic complexity. *EMBO Rep* 2:986–991.
12. Mattick JS, Makunin IV (2006) Non-coding RNA. *Hum Mol Genet* 15:R17–29.
13. Li Z, et al. (2008) A microRNA signature for a BMP2-induced osteoblast lineage commitment program. *Proc Natl Acad Sci USA* 105:13906–13911.
14. Luzi E, et al. (2008) Osteogenic differentiation of human adipose tissue-derived stem cells is modulated by the miR-26a targeting of the SMAD1 transcription factor. *J Bone Miner Res* 23:287–295.
15. Mizuno Y, et al. (2008) miR-125b inhibits osteoblastic differentiation by down-regulation of cell proliferation. *Biochem Biophys Res Commun* 368:267–272.
16. Kobayashi T, et al. (2008) Dicer-dependent pathways regulate chondrocyte proliferation and differentiation. *Proc Natl Acad Sci USA* 105:1949–1954.
17. Davis BN, Hilyard AC, Lagna G, Hata A (2008) SMAD proteins control DROSHA-mediated microRNA maturation. *Nature* 454:56-61.
18. Tuddenham L, et al. (2006) The cartilage specific microRNA-140 targets histone deacetylase 4 in mouse cells. *FEBS Lett* 580:4214–4217.
19. Harfe BD, McManus MT, Mansfield JH, Hornstein E, Tabin CJ (2005) The RNaseIII enzyme Dicer is required for morphogenesis but not patterning of the vertebrate limb. *Proc Natl Acad Sci USA* 102:10898–10903.
20. Watanabe T, et al. (2008) Dnm3os, a non-coding RNA, is required for normal growth and skeletal development in mice. *Dev Dyn* 237:3738–3748.
21. Sugatani T, Hruska KA (2007) MicroRNA-223 is a key factor in osteoclast differentiation. *J Cell Biochem* 101:996–999.
22. Katagiri T, et al. (1994) Bone morphogenetic protein-2 converts the differentiation pathway of C2C12 myoblasts into the osteoblast lineage. *J Cell Biol* 127:1755–1766 .
23. Hohjoh H, Fukushima T (2007) Marked change in microRNA expression during neuronal differentiation of human teratocarcinoma NTera2D1 and mouse embryonal carcinoma P19 cells. *Biochem Biophys Res Commun* 362:360–367.
24. Kim HK, Lee YS, Sivaprasad U, Malhotra A, Dutta A (2006) Muscle-specific microRNA miR-206 promotes muscle differentiation. *J Cell Biol* 174:677–687.
25. Politz JC, Zhang F, Pederson T (2006) MicroRNA-206 colocalizes with ribosome-rich regions in both the nucleolus and cytoplasm of rat myogenic cells. *Proc Natl Acad Sci USA* 103:18957–18962.
26. Rao PK, Kumar RM, Farkhondeh M, Baskerville S, Lodish HF (2006) Myogenic factors that regulate expression of muscle-specific microRNAs. *Proc Natl Acad Sci USA* 103:8721–8726.
27. Rosenberg MI, Georges SA, Asawachaicharn A, Analau E, Tapscott SJ (2006) MyoD inhibits Fstl1 and Utrn expression by inducing transcription of miR-206. *J Cell Biol* 175:77–85.
28. Sweetman D, et al. (2008) Specific requirements of MRFs for the expression of muscle specific microRNAs, miR-1, miR-206, and miR-133. *Dev Biol* 321:491–499.
29. Sambrook J, Fritsch EF, Maniatis T (1989) in *Molecular Cloning: A Laboratory Manual* (Cold Spring Harbor Laboratory, Cold Spring Harbor, NY), pp 7.2–7.87.
30. Reue K (1998) mRNA quantitation techniques: Considerations for experimental design and application. *J Nutr* 128:2038–2044.
31. McKinsey TA, Zhang CL, Olson EN (2002) Signaling chromatin to make muscle. *Curr Opin Cell Biol* 14:763–772.
32. Krek A, et al. (2005) Combinatorial microRNA target predictions. *Nat Genet* 37:495–500.
33. Lewis BP, Burge CB, Bartel DP (2005) Conserved seed pairing, often flanked by adenosines, indicates that thousands of human genes are microRNA targets. *Cell* 120:15–20.
34. Chung DJ, et al. (2006) Low peak bone mass and attenuated anabolic response to parathyroid hormone in mice with an osteoblast-specific deletion of connexin43. *J Cell Sci* 119:4187–4198.
35. Lecanda F, et al. (2000) Connexin43 deficiency causes delayed ossification, craniofacial abnormalities, and osteoblast dysfunction. *J Cell Biol* 151:931–944.
36. Tiso N, et al. (1997) Fine mapping of five human skeletal muscle genes: alpha-tropomyosin, beta-tropomyosin, troponin-I slow-twitch, troponin-I fast-twitch, and troponin-C fast. *Biochem Biophys Res Commun* 230:347–350.
37. Dacquin R, Starbuck M, Schinke T, Karsenty G (2002) Mouse alpha1(I)-collagen promoter is the best known promoter to drive efficient Cre recombinase expression in osteoblast. *Dev Dyn* 224:245–251.
38. Mitchell JA, Ou C, Chen Z, Nishimura T, Lye SJ (2001) Parathyroid hormone-induced up-regulation of connexin-43 messenger ribonucleic acid (mRNA) is mediated by sequences within both the promoter and the 3′untranslated region of the mRNA. *Endocrinology* 142:907–915.
39. Caplan AI, Pechak DG (1987) in *Bone and Mineral Research*, ed Peck WA (Elsevier, New York), pp 117–183.
40. Walden TB, Timmons JA, Keller P, Nedergaard J, Cannon B (2009) Distinct expression of muscle-specific MicroRNAs (myomirs) in brown adipocytes. *J Cell Physiol* 218:444–449.
41. Care A, et al. (2007) MicroRNA-133 controls cardiac hypertrophy. *Nat Med* 13:613–618.
42. Sato S, et al. (2007) Central control of bone remodeling by neuromedin U. *Nat Med* 13:1234–1240.
43. Saito K, et al. (2006) Specific association of Piwi with rasiRNAs derived from retrotransposon and heterochromatic regions in the Drosophila genome. *Genes Dev* 20:2214–2222.
44. Obernosterer G, Martinez J, Alenius M (2007) Locked nucleic acid-based *in situ* detection of microRNAs in mouse tissue sections. *Nat Protoc* 2:1508–1514.

Clin Orthop Relat Res (2009) 467:3087–3095
DOI 10.1007/s11999-009-0976-6

Stimulation of Ectopic Bone Formation in Response to BMP-2 by Rho Kinase Inhibitor

A Pilot Study

Hideki Yoshikawa MD, PhD, Kiyoko Yoshioka, Takanobu Nakase MD, PhD, Kazuyuki Itoh MD, PhD

Published online: 17 July 2009

Abstract The small GTPase Rho and Rho-associated protein kinase (Rho kinase, ROCK) signal participates in a variety of biological functions including vascular contraction, tumor invasion, and penile erection. Evidence also suggests Rho-ROCK is involved in signaling for mesenchymal cellular differentiation. However, whether it is involved in osteoblastic differentiation is unknown. We therefore asked whether Rho-ROCK signaling participates in recombinant human bone morphogenetic protein (rhBMP-2)-induced osteogenesis both in vitro and in vivo. Continuous delivery of a specific ROCK inhibitor (Y-27632) enhanced ectopic bone formation induced by rhBMP-2 impregnated into an atelocollagen carrier in mice without affecting systemic bone metabolism. Treatment with Y-27632 also enhanced the osteoblastic differentiation of cultured murine neonatal calvarial cells. These effects were associated with increased expression of BMP-4 gene. Expression of a dominant negative mutant of ROCK in ST2 cells promoted osteoblastic differentiation, while a constitutively active mutant of ROCK attenuated osteoblastic differentiation and the ROCK inhibitor reversed this phenotype. Thus, ROCK inhibits osteogenesis, and a ROCK inhibitor in combination with the local delivery of rhBMP/collagen composite may be clinically applicable for stimulating bone formation.

Each author certifies that he or she has no commercial associations (eg, consultancies, stock ownership, equity interest, patent/licensing arrangement, etc) that might pose a conflict of interest in connection with the submitted article. This work is supported in part by Grant-in-Aid for Scientific Research from the Ministry of Education, Science, Sports, Culture and Technology of Japan, as well as by research grants from the Yamanouchi Foundation for Research on Metabolic Disease.
Each author certifies that his or her institution has approved the animal protocol for this investigation and that all investigations were conducted in conformity with ethical principles of research.
This work was performed at Osaka Medical Center for Cancer and Cardiovascular Diseases, Osaka, Japan.

H. Yoshikawa, K. Yoshioka, K. Itoh (✉)
Department of Biology, Osaka Medical Center for Cancer and Cardiovascular Diseases, 1-3-2 Nakamichi, Higashinari-ku, Osaka 537-8511, Japan
e-mail: itou-ka@mc.pref.osaka.jp

H. Yoshikawa, T. Nakase
Department of Orthopedic Surgery, Osaka University Medical School, Suita, Osaka, Japan

Introduction

Bone morphogenetic protein (BMP), a potent inducer of bone formation both in vitro and in vivo, promotes the differentiation of mesenchymal cells into osteoblasts and is believed responsible for fracture repair or regeneration of bone defects [,]. Implantation of BMP can elicit new bone formation both in orthotopic and heterotopic sites [,], and is used as a bone graft substitute in the clinical setting [, ,]. Although it is now possible to generate recombinant human BMPs for medical use, more than 1.5 mg/kg of the recombinant protein has been required for bone induction in primates [,], probably due to their reduced capability for tissue regeneration. Therefore, the major challenge still remains in the enhancement of its activity to induce early and optimal bone formation in humans.

The biological activity of BMP is regulated by various growth factors or cytokines through several intracellular signaling pathways, including Smad protein signaling [,]. To explore the mechanism for BMP-induced bone formation, we developed an in vivo experimental model

system for the local delivery of recombinant human BMP-2 (rhBMP-2) impregnated in pepsin-digested Type I collagen [29]. With this model we can reproducibly induce ectopic bone and assess bone formation quantitatively in any wild-type or transgenic mice [17, 34]. Our studies suggest granulocyte colony-stimulating factor (G-CSF) [17], basic calponin [34], and TNP-470 [23] (a synthetic anti-angiogenic agent) inhibit BMP-induced bone formation. Using this in vivo system, it should be possible to search for stimulators of BMP-induced bone formation.

The small GTPase Rho and its target Rho-associated protein kinases (Rho kinase, p160ROCK) [9, 18, 19] control cell adhesion [10] and motility [35] through reorganization of the actin cytoskeleton and regulation of actomyosin contractility [3] in a number of cellular processes, including vascular contraction [31], tumor invasion [12], penile erection [2], and apoptosis [4]. Further, several lines of evidence indicated that Rho-ROCK signaling also has been involved in cellular transformation. NIH3T3 cells expressing active Rho or ROCK representing enhanced transformation capability and a specific inhibitor (Y-27632 [31]) for ROCK-inhibited Rho, ROCK, or even Ras-induced cellular transformation [28]. This accumulating evidence suggests Rho-ROCK signaling is also involved as molecular switch for lineage-specific cellular differentiation. However, little is known about the involvement of this signaling for the mesenchymal cellular differentiation including osteogenesis.

To this end, we asked: (1) Does ROCK inhibitor enhance BMP-induced bone formation in vivo? (2) What kind of cells migrate to the BMP/atelocollagen pellets to induce bone formation in vivo? (3) Does ROCK inhibitor itself enhance osteogenic differentiation of primary cultured calvaria cells in vitro? (4) What is the mechanism for ROCK inhibitor-induced osteogenic differentiation? (5) Does ectopic expression of dominant negative ROCK enhance osteoblastic differentiation and does ectopic expression of active ROCK inhibit it?

Materials and Methods

In order to answer our five study questions, we carried out the experiments in the following order. First, we assayed ectopic bone formation using BMP/atelocollagen pellets with or without ROCK inhibitor in mice. Next, we analyzed the phenotype of the cells that migrated to the BMP/atelocollagen ossicles using an in situ hybridization method. We then examined the effects of ROCK inhibitor on osteoblastic differentiation in vitro using primary culture of osteoblast from newborn mice. We then analyzed the mechanism of Rho-ROCK signaling on the expression of BMP transcript (RNA) in mesenchymal ST2 cells in vitro. Finally, we confirmed the inhibitory role of ROCK on the osteogenesis by the introduction and expression of ROCK mutants in ST2 cells.

BMP/atelocollagen pellets containing 5 μg of rhBMP-2 (kindly provided by Genetics Institute, Cambridge, MA, through Astellas Pharma Inc., Tokyo, Japan) and 3 mg of atelocollagen (Nitta Gelatin, Osaka, Japan) were implanted into a dorsal subfascial pocket of eight 5-week-old male ICR mice. Six mice were sacrificed at 4 days, six at 1 week, and six at 2 weeks after implantation of the pellets. Recovered ossicles were examined radiographically with a soft xray apparatus (Softex Type SM, Osaka, Japan) and histologically. Calcium content in the ossicles was quantified as follows: the ossicles were defatted with trichloroethylene and methanol (1:1) for 24 hours, dried by evaporation, and then decalcified with 1 mL of 0.6 N HCl for 24 hours. The calcium content of the HCl-supernatants was measured using the calcium C-test (Wako Pure Chemicals, Osaka, Japan). Tissue preparation and in situ hybridization were carried out as previously described [7, 25]. Harvested tissues were fixed in 4% paraformaldehyde, dehydrated in an ethanol series, and embedded in paraffin wax. Six sections 4 μm thick were hybridized with digoxigenin-labeled antisense and sense cRNA probes for mouse BMP-4 [ ], mouse osteopontin [26], and mouse a1 chain of procollagen Type I [25]. Hybridization proceeded at 50°C for 16 hours with 0.5 mg/mL of each RNA probe in hybridization buffer (50% deionized formamide, 10% dextran sulfate, 1 × Denhardt's solution, 4 × SSC, 3 mg/mL of Escherichia coli tRNA), followed by washing and RNase treatment (10 μg/mL) at 37°C for 30 minutes. Hybridized probes were detected using a nucleic acid detection kit (Roche Diagnostic, Japan) according to the manufacturer's instructions. Sections hybridized with sense probes showed no positive signals.

Tetracycline double-labeling analysis was performed using six undecalcified sections of the tissues. Tetracycline injection (30 mg per kg body weight) was performed at 2 and 4 days (for tibia), or at 3 hours (for ossicles) before sacrifice of the animals. The tibia and the ectopic ossicles were recovered, fixed in 70% methanol, stained in Villanueva bone stain, dehydrated in increasing concentrations of ethanol, defatted in xylene, and embedded in methyl methacrylate. Histomorphometric analyses were performed with a semiautomatic digitizing image analyzer. The system consisted of a light or epifluorescent microscope and a digitizing pad coupled to a computer with histomorphometric software (System Supply Co., Nagano, Japan).

Twenty to thirty primary cultures of murine calvarial cells were obtained from the twenty to thirty neonatal ICR mice 1 day after birth by sequential collagenase/trypsin digestion [34]. The mouse bone marrow-derived stromal

cell line ST2 (RCB0224) was obtained from the Riken Cell Bank (Tsukuba, Japan). Neonatal murine calvarial cells were maintained in α-MEM containing 10% FCS, and ST2 cells were maintained in RPMI1640 containing 10% FBS (Invitrogen).

To determine ALP activity, ST2 cells were split, plated at a density of 1×10^4 cells per cm^2 and cultured for 24 hours in growth medium on 48 plastic culture dishes. MC3T3-E1 cells were plated at a density of 1×10^5 cells per cm^2 and cultured for 24 hours in growth medium. In some experiments, ST2 cells were cultured in α-modified minimum essential medium (a-MEM, Invitrogen) containing 10% FBS on a collagen I-coated culture dish (Celltight C-1, Sumitomo Bakelite Co., Japan). rhBMP-2 and/or Y-27632 were added at various concentrations to the subconfluent cultures in the presence of growth medium. The culture medium was changed daily and the cells were further cultured for the indicated time period. After removing the culture media, cells were washed with PBS and sonicated for 10 seconds at 0°C in 20 mM Tris-HCl, pH 7.5, 0.1% Triton X-100, 10 μg/ml leupeptin, 10 μg/ml aprotinin, and 1 mM phenylmethylsulfonyl fluoride. The ALP activity was determined using *p*-nitrophenyl-phosphate as a substrate according to the Kind and King's method (Wako Pure Chemicals).

Primary culture of calvarial cells was plated onto four 12-well plates at the density 2×10^4 cells/cm^2 with α-MEM containing 10% FBS. At 18 hours after plating, the culture media were replaced α-MEM containing 5% FBS, 5 mM β-glycerol phosphate (Sigma), and 100 μg/mL ascorbic acid without or with 3, 5, 10, 20, 30 μM Y-27632. Cultured for 16 days, cells were fixed for 30 minutes with 3.7% formaldehyde/PBS at RT. After washing with PBS, nodules were stained with 1% alizarin red S (Sigma) at pH 6.0 [ ].

To measure the level of BMP transcript, 39 samples (3 replicates for 13 experiments: zero days; and 1, 2, and 3 days for two Y-27632 treatment and two doses rhBMP-2) of total RNA were prepared from culture cells using Trizol reagent (Life Technologies). RNA was denatured by the treatment with 1.1 M glyoxal, run in a 1.2% agarose gel, and then transferred for 8 hours by capillary action to a Hybond-N+ membrane (Amersham, UK) and UV cross-linked with a cross-linker (1200 watts) (Stratagene). A [α-^{32}P] dCTP-labeled probe was made with Multiprime DNA labeling systems (Amersham). The membrane was hybridized for 2 hours at 65°C with the Rapid-hyb buffer (Amersham) containing the radioactive probe. After hybridization, the filters were washed twice for 10 minutes at room temperature in 0.1% SDS-2 × SSC and twice for 30 minutes at 65°C in 0.1% SDS-0.2 × SSC. Processed filters were analyzed using a FLA-2000 image analyzer (Fujifilm Co, Japan). Full-length cDNA for murine BMP-4 was synthesized by RT-PCR. The reverse transcriptase reaction was carried out using random hexamers and Moloney murine leukemia virus reverse transcriptase (Takara, Otsu, Japan). The PCR reaction profile included 30 cycles of denaturation for 1 minute at 95°C, annealing for 1 minute at 50°C and extension for 1 minute at 72°C using *Pfx* DNA polymerase (Invitrogen). The PCR product was separated by agarose gel electrophoresis, subcloned into pCR-ScriptSK(+) vector (Stratagene), and sequenced with an ABI PRISM model 377 sequencer (Perkin Elmer). The 1.2 k base pairs of murine full-length BMP-4 cDNA was used for a specific probe for RNA blot. 3′-UTR region of murine cbfa-1 gene was used for RNA blotting as previously reported [ ].

cDNAs encoding the catalytic domain of ROCK (amino acids, 1 to 477) and the catalytic domain with a Lys105-> Ala mutation in the ATP-binding region (KD) [ ], each tagged at the NH2-terminus with the FLAG epitope, were inserted into the Kpn I and Xba I sites of the pcDNA3 vector (Invitrogen). ST2 cells were transiently transfected with the resulting expression vectors by Lipofectamine Plus reagent (Invitrogen) following the manufacturer's protocol.

Data were expressed as means ± SEM in all figures. We determined the difference in ossicle wet weight, calcium content, and all bone histomorphometric parameters by the ROCK inhibitor in vivo using Student's t-test. We determined the difference in ALP activity and osteocalcin production in cultured calvaria cells by the ROCK inhibitor in vitro using Student's t-test. We determined the difference in BMP-4 transcript and ALP activity by the ROCK inhibitor or expression of ROCK mutants in ST2 cells in vitro using Student's t-test. All statistical analyses were performed using a JMP8.0 software package (SAS Institute Inc, NC).

Results

The ossicles induced by the rhBMP-2/collagen composites with Y-27632 treatment for 2 weeks were larger, contained reddish-colored bone marrow and highly dense xray-absorbed calcium when compared with those induced in phosphate buffered saline (PBS)-treated control mice (Fig. A–B). Microscopic observations (Fig. C–F) revealed the normal bone formation with fully mature bone marrow and no obvious difference apart from bone volume between two groups. The concentrations of the inhibitor in the serum (1 ± 0.3 μM for 15 mg/2w, 3.5 ± 0.7 μM for 50 mg/2w) and the tissue (28.9 ± 12.6 μM for 15 mg/2w, 70.3 ± 18.6 μM for 50 mg/2w) were positively correlated with the bone wet weight (Fig. G) or calcium content (Fig. H).

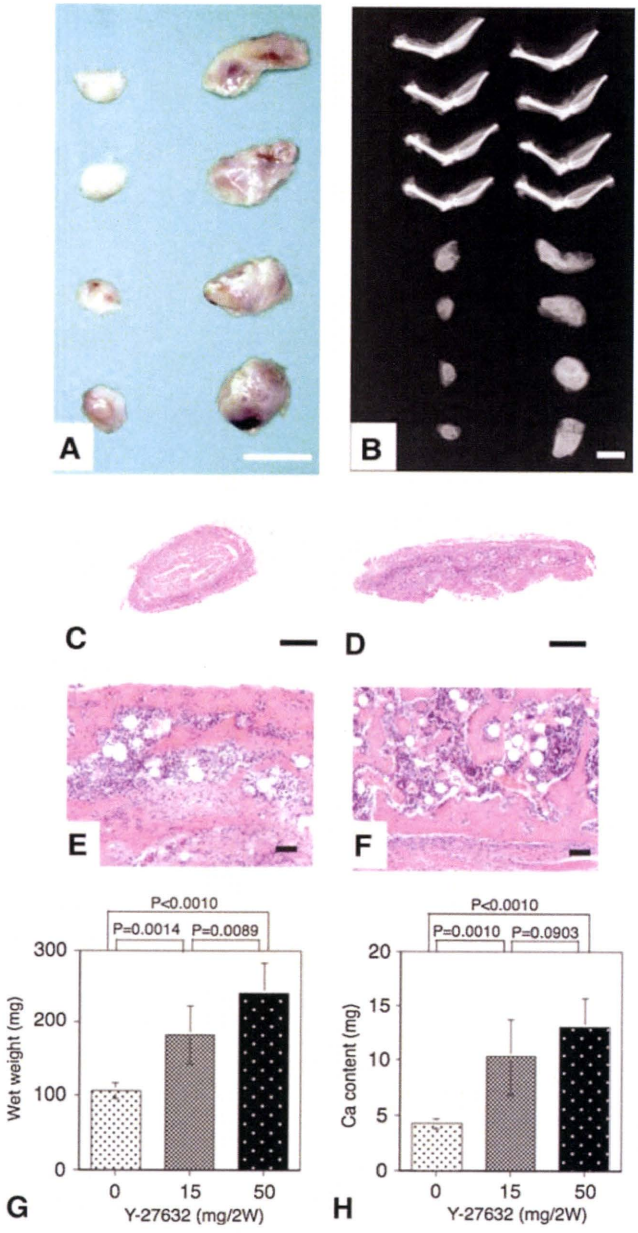

Fig. 1A–H ROCK inhibitor stimulated the ectopic bone formation in vivo induced by BMP. (**A**) Macroscopic pictures of ectopic ossicles 2 weeks after implantation of BMP/atelocollagen composites containing 5 μg of rhBMP-2, in control (left) and Y-27632-treated (right) mice are shown. Scale bar, 10 mm. (**B**) Radiographs of the ossicles and the bones of the lower extremities in control (left) and Y-27632-treated (right) mice are shown. Scale bar, 10 mm. Cross-sections of the ossicles in (**C**) control and (**D**) Y-27632-treated mice are shown (Stain, hematoxylin and eosin; original magnification ×10; scale bar, 1 mm). Calcified trabeculae and maturated bone marrow can be seen in both (**E**) control and (**F**) Y-27632-treated mice (Stain, hematoxylin and eosin; original magnification ×10; scale bar, 100 μm). (**G**) Wet weight of each ossicle is present (mean ± SEM, n = 4). (**H**) Calcium content of each ossicle is present (mean ± SEM, n = 4) (in the absence of Y-27632).

The treatment of ROCK inhibitor did not affect ($p > 0.1$) the three osteoblastic and three osteoclastic parameters in the tibia (Table 1). In the ossicles, one bone-formation parameter (BV/TV) increased ($p = 0.027$) and two bone absorption parameters (Oc.S/BS and N.Oc/BS) decreased ($p = 0.019$ and 0.011, respectively) by the treatment with ROCK inhibitor. Taken together, the treatment of ROCK inhibitor per se did not affect the general bone metabolism in the mice, and the stimulatory effects of the inhibitor on the osteogenesis were restricted to the BMP-2/collagen composite.

Table 1. Histomorphometric analysis of tibia and ossicles in the mice treated with ROCK inhibitor (Y-27632) (values expressed as mean ± SD)

Tibia			
Variable	Control	Y-27632	p Value
BV/TV (%)	12.48 ± 1.37	13.01 ± 1.47	0.301
Ob.S/BS (%)	8.81 ± 2.33	8.18 ± 1.40	0.673
BFR/BS (mm^3/mm^2/year)	0.0741 ± 0.025	0.0709 ± 0.0243	0.860
ES/BS (%)	32.8 ± 4.35	34.4 ± 3.22	0.569
Oc.S/BS (%)	7.99 ± 2.36	8.20 ± 1.84	0.863
N.Oc/BS (number/mm)	2.16 ± 0.54	2.16 ± 0.55	0.988
Ossicles			
Variable	Control	Y-27632	p Value
BV/TV (%)	9.77 ± 4.55	26.15 ± 6.39	0.027*
Ob.S/BS (%)	5.86 ± 3.32	9.72 ± 4.41	0.141
BFR/BS (mm^3/mm^2/year)	0.418 ± 0.062	0.480 ± 0.111	0.397
ES/BS (%)	93.1 ± 3.82	85.5 ± 7.21	0.57
Oc.S/BS (%)	35.5 ± 3.74	28.1 ± 4.79	0.019*
N.Oc/BS (number/mm)	10.08 ± 1.17	6.78 ± 2.12	0.011*

BV/TV = bone volume/total volume; Ob.S/BS = osteoblast surface/bone surface; and BFR/BS = bone formation rate/bone surface are osteoblastic parameters. ES/BS = erosion surface/bone surface; Oc.S/BS = osteoclast surface/bone surface; and N.Oc/BS = number of osteoclast/bone surface are osteoclastic parameters.

* $p < 0.05$.

On Day 4 postimplantation, numerous mesenchymal cells were recruited adjacent to BMP/collagen implants in Y-27632-treated mice (Fig. 2A and C). Surrounding mesenchymal cells were separated from BMP/collagen pellet by loose connective tissue in PBS-treated mice (Fig. 2E and G). In situ hybridization analysis revealed the transcripts for BMP-4 (Fig. 2B and D) were localized in mesenchymal cells close to the BMP/collagen implant in Y-27632-treated mice. However, the signals for BMP-4 transcripts were marginal in PBS-treated mice (Fig. 2F and H). The migrating cells were also positive for Type I collagen and osteopontin, and negative for tartrate-resistant acid phosphatase (TRAP) (Fig. 2I–L).

In murine calvarial cultures, the ROCK inhibitor not only stimulated ALP activity and osteocalcin production in